An Honours Programme Research on

The interaction between the canonical Wnt pathway and the mTOR pathway in canine mammary tumor cells

By R.R. Steenlage
3674290

Supervised by
Ing. E.P.M. Timmermans-Sprang
Dr. Ir. J.A. Mol

Department of Clinical Sciences of Companion Animals
Faculty of Veterinary Medicine, Utrecht University, The Netherlands

2014-2015

Table of Contents

General abstract

Background: Mammary tumors are the most common neoplasms in intact bitches with an estimated life-time risk to develop of 1:4. About 50% of these tumors are malignant and one-third of these may form life-threatening distant metastases. Also in humans breast cancer is a very common disease with a life-time risk of about 1:8. The initial hormone dependency and the common pathways involved in cell proliferation and migration, such as Wnt and PI3K signaling in both human and canine mammary carcinomas underscore the relevance of the research in canine mammary cancer. The main problem in breast cancer treatment is the recurrence of tumor growth and metastases. Tumor cells with stem cell properties such as a phenotypical epithelial mesenchymal transition (EMT) and elevated activity of the canonical Wnt pathway play an important role in regrowth and metastasis. In previous research a subset of canine mammary cell lines were shown to have elevated ligand-independent canonical Wnt activity. This was associated with enhanced expression of EGFR, HER2 and HER3 receptors and loss of PTEN expression suggesting a role for activation of the PI3K/mTor pathway. However, inhibition with a specific mTOR inhibitor or a dual PI3K/mTOR inhibitor resulted in further increased Wnt activity that appeared to be sensitive to inhibition of the also through EGFR and HER2/3 activated SRC.

Aim: The aim of this research project was to further study the role of SRC inhibition on basal Wnt activity and inhibition of in vitro migration as a surrogate marker for metastasis. In a second part the role of HER2 and HER3 were further investigated by selective inhibition of HER2 and HER3 expression.

Methods: Using a panel of specific inhibitors related to the previously used SRC inhibitor SRC-I1 their effect was studied on two canine mammary cell lines, one with elevated basal Wnt activity and one with absent Wnt activity. The effects of the inhibitors on cell viability were measured by MTT assay, on the basal Wnt activity using TCF-reporter constructs and on cell migration using scratch assays. In the second study expression of HER2 or HER3 was selectively inhibited using specific siRNAs. The effects of these siRNAs were studied on protein expression by Western blot, on Wnt activity using reporter assays, and on target gene expression using qPCR.

Results: In general no differences in sensitivity for a decrease in viability were found between the two cell lines with the exception of a higher sensitivity of the high basal Wnt cell line for Aurora kinase A inhibition. This was, however, not associated with a decreased Wnt activity which was sensitive to SRC inhibitors SRC-I1 and PP2 but also to an IGF-1R inhibitor. In addition, migration appeared to be sensitive to the SRC inhibitors SRC-I1 and PP2. These data confirm the central role of SRC activation in the enhanced basal Wnt activity and metastatic properties. The remaining question was if the overexpression of HER2 and HER3 were causing the enhanced Wnt activity. Selective inhibition of HER2 or HER3 expression, using specific siRNAs, however did not unequivocally show overexpression of HER2 or HER3 as the cause of Wnt pathway activation.

Conclusion: Further evidence is presented for a central role of SRC in Wnt activation and migratory properties of the canine mammary cell line used. The role of HER2 and HER3 remain, however, inconclusive. This may be caused by incomplete knockdown or the necessity of inactivating both genes at the same time. In addition, a role for the EGFR may exist and needs further research.

1. General introduction

1.1 Mammary tumors

Mammary tumors are tumors of the mammary gland. The mammary gland is a modified apocrine sweat gland which distinguishes mammals from all other species. Dogs mainly develop five pairs of mammary glands: two thoracic, two abdominal and one inguinal pair. The mammary gland consists of a stromal and an epithelial compartment. The stromal part comprises blood vessels, lymphatics, fibrous tissue and fat. The epithelial compartment forms the ductal network and consists of alveoli, ducts and myoepithelial cells. (1-3)

The development of the mammary gland is regulated by hormonal factors that govern the action of a great number of specific growth factors, receptors and other proteins (Fig. 1). (4)

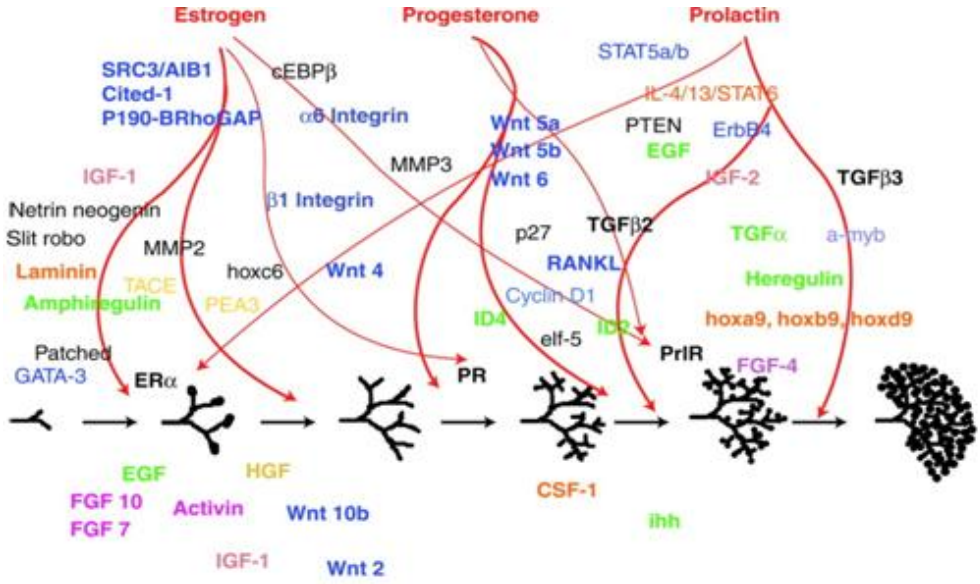

Figure 1. Factors involved in mammary gland development. Many genes are important in mammary gland development, which are summarized in the scheme. Adapted from Brisken C. *et al.* (2010) (4)

In non-lactating female dogs, and in male dogs at all time, the mammary gland consists predominantly of stroma. The mammary gland uniquely forms after birth from an initial 'anlage' towards an extensive network of ducts and alveoli that interacts with the stromal compartment. In the lactating state, the mammary gland changes in a compound tubuloalveolar system. Cells in the alveoli contract in the presence of oxytocin and in response to suckling, so that the milk is squeezed into the larger ducts. (1-3) These changes are hormone-dependent and the cyclic activity of the mammary gland is characterized by development and regression phases. (5)

So, during a mammalian life the mammary gland has the potential to undergo a lot of changes in size, composition, activity and other characteristics in comparison with other organs. Therefore, it is not surprisingly that in the regulation of these events, the mammary gland can grow in an uncontrolled way leading to the formation of tumors.

Mammary tumors are the most common neoplasms in intact bitches. More than 40% of all neoplasms in female dogs are mammary tumors. (6) About 50% of canine mammary tumors (CMTs) in the bitch are malignant, and most of them are carcinomas. The caudal abdominal and inguinal mammary glands are mostly affected, and most dogs develop multiple tumors. (6)(7)(8)

The risk of development of mammary tumors in the bitch increases after each estrous cycle. Ovari(ohyster)ectomy (OVX) reduces the incidence of CMTs. If performed before the first estrous cycle the risk of developing a mammary tumor is 0.5%, 8% when performed after the first cycle and over 26% after more estrous cycles. (9) However, there are still many countries where OVX is not performed routinely. For example, regions such as Spain and Scandinavia, where OVX is not performed routinely, the incidence of CMTs is much higher than in countries where OVX is common practice. (6)

The most common and preferred treatment of mammary tumors is surgery. Dogs with benign tumors and around 50% of dogs with malignant CMTs can be cured with surgery alone. The remaining 50% of dogs with malignant CMTs already show metastases at the time of operation, leading to a further progress of the disease. These dogs may benefit from adjuvant therapy, such as chemotherapy, radiotherapy, anti-Cox-2 treatment and hormonal therapy. (6) However, these adjuvant therapies are not performed routinely in each veterinary practice, making metastases of CMTs still a big problem to deal with in veterinary medicine.

In humans, breast cancer is also a very common disease. It is even the most commonly diagnosed cancer. Unless improvements in the understanding of breast cancer and the development of several treatment methods, breast cancer causes still the most cancer-related deaths in women. Death is usually due to metastasis. Metastasis occurs in approximately 25% to 50% of all breast cancers. After the diagnosis metastasis is made, the 5 year survival rate is generally less than 25%. (10)(11)

For several reasons, CMTs are useful models for human breast cancer research. First, mammary tumors in dogs develop spontaneously and naturally, capturing the essence of human breast cancer. Second, dogs share the same environment as humans, and are therefore exposed to many of the same risk factors. (12) Furthermore, there are similarities in biology and signaling pathways, for example the Wnt pathway. Also anatomic and clinical similarities between both species are documented, and also similar treatment schemes are used. (13)

Different classification methods of CMTs and human breast tumors are used. For example, the World Health Organization (WHO) uses a classification based on histology, morphology and prognostic factors. (6) Also molecular-based classifications are described. Gene expression profiling has demonstrated five subtypes of carcinomas: two hormone (estrogen and/or progesterone) receptor positive types (called luminal like-A and luminal like-B), and three receptor negative types (subdivided in the human epidermal growth factor receptor-2 (HER2) expressing, basal-like and normal like). When focusing on the expression of hormone receptors and HER2, these subtypes can be regrouped into three subtypes: the hormone-dependent type, the HER2 positive (HER2+) type and the triple negative (TNBC) type.
Also the incidence of the three subtypes is quite the same for canine and human breast cancer. In both species most tumors are hormone receptor positive (about 65%). Of the remaining 35%, the majority is HER2+ (around 20%) in humans, whereas the majority in dogs is TNBC (approximately 25%). (5)(9)(14-17)

1.2 Epithelial mesenchymal transition

As long as tumors remain at the site of origin, surgical excision and, if needed, adjuvant therapy is successful in the treatment of most cancers. As previously mentioned, one of the main problems in breast cancer is dealing with metastasis. Epithelial mesenchymal transition (EMT) plays an important role in the metastatic process.

Epithelial cells are well organized cells which are closely attached to each other and the basement membrane with tight junctions. Mesenchymal cells do not possess these intercellular junctions, what makes them more motile than the epithelial cells. EMT is the process where epithelial cells, which are not motile themselves, become motile cells such as the mesenchymal cells (Fig. 2). This phenomenon is especially seen in primary tumor cells which have a breast cancer stem cell (BCSC) phenotype. (18)(19)

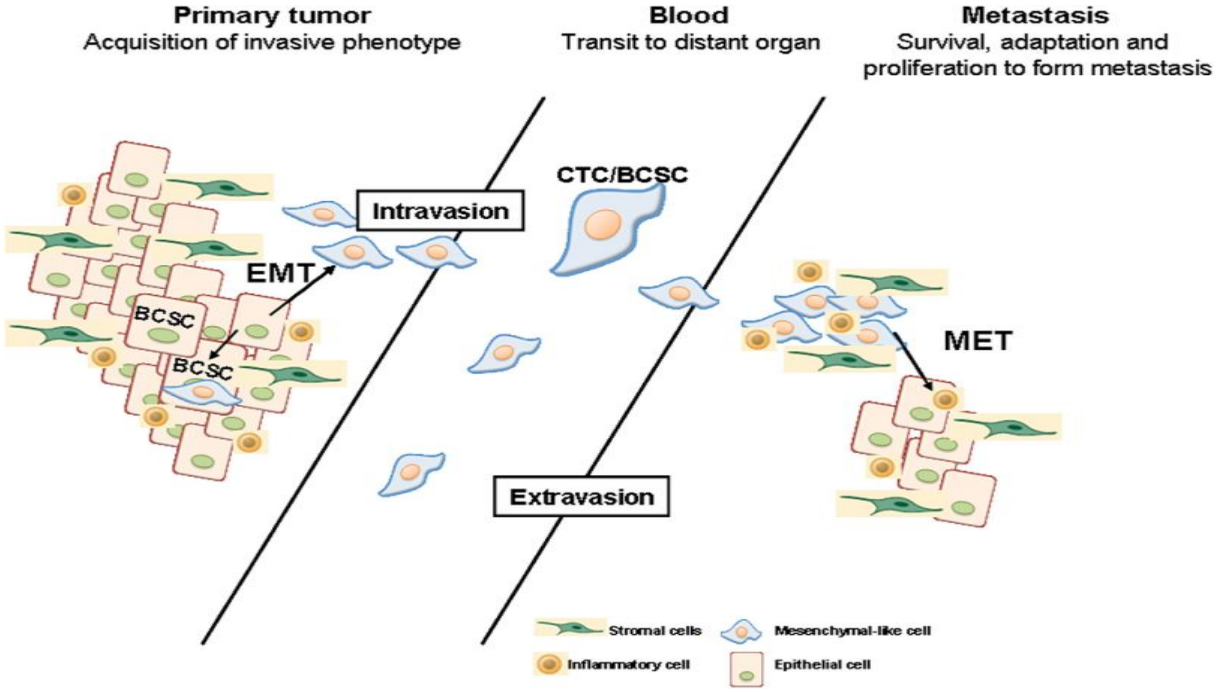

Figure 2. Involvement of EMT in the metastatic process. Epithelial cells become motile cells such as mesenchymal cells, making them able to transit to distant organs where they revert to their epithelial phenotype due to MET. BCSC, breast cancer stem cell; CTC, circulating tumor cell; EMT, epithelial mesenchymal transition; MET, mesenchymal epithelial transition. Adapted from Foroni C. et *al*. (2012). (18)

The epithelial cells lose their intercellular junctions to release them from the surrounding tissue. In addition, their cytoskeleton alters to make them able to move through the extracellular matrix (ECM). (18)(19). This transition makes the epithelial cells able to intravasate the bloodstream, to be carried away with the circulation and finally to extravasate the vessels and spread into distant sites where they can revert to their epithelial phenotype due to a mesenchymal epithelial transition (MET). The last step in this metastatic process is the formation of new tumors in the invaded tissues. (19)(20)

Besides the metastatic process, EMT is also linked to resistance to chemotherapy. Together with the strong motile capacities, the cells arisen from EMT also have stem cell-like characteristics. These cells are intrinsically resistant to therapy. (18)(21) There are several signaling pathways involved in the EMT process, including TGF-b, Wnt, Notch, NFκB and ERK/MAPK pathways. (22) Because this project focuses on the Wnt pathway, this pathway and its role in the oncogenesis of CMTs will be further explained.

1.3 The Wnt pathway

The Wnt pathway plays a role in physiological development by controlling the development of the mammary gland during embryogenesis, pregnancy and lactation, but also in oncogenesis. (23)(24) There are two Wnt signaling pathways known; a canonical and a non-canonical pathway. Both pathways will be discussed below. Because this project mainly focuses on the canonical pathway, this pathway is more extensively described than the non-canonical pathways. (25)

1.3.1 Wnt proteins and the Frizzled receptor

The Wnt signaling pathway was first described in *Drosophila*, where the gene Wnt was found as the initiator of the absence of wings. As a result, the gene was named ''wingless''. Later on, there was a mutation found in a mouse gene, which caused malignant alterations in mammary tissues. The sequence was called ''int''. It was found that the *Drosophila* and mouse genes were homologous, so the genes were combined to form the name "Wnt". (26) Wnt proteins are secreted glycoproteins and there are 19 mammalian Wnt proteins known. (27)

Wnt proteins bind to the Frizzled receptor. Each receptor includes an N-terminal signal peptide, an extracellular cysteine-rich domain (CRD), a seven-pass transmembrane domain, and an intracellular C-terminal PDZ domain. The CRD allows interaction of the Frizzled receptor with Wnt proteins, whereas the PDZ domain allows the transduction of Wnt signals by interacting with the Dishevelled protein (DVL). (28)

Binding of Wnt to the CRD of the Frizzled receptor does not lead to an effect itself. Co-receptors, such as the low-density-lipoprotein-related protein5/6 (LRP5/6), are also required to generate a Wnt signal. (29)(30) When Wnt has bound to the receptor complex, the signal is transduced to DVL. Hereafter, the Wnt signal can branch into the canonical or the non-canonical pathway. (29)

1.3.2 The canonical pathway

The canonical pathway is also known as the Wnt/β-catenin dependent pathway. (31)

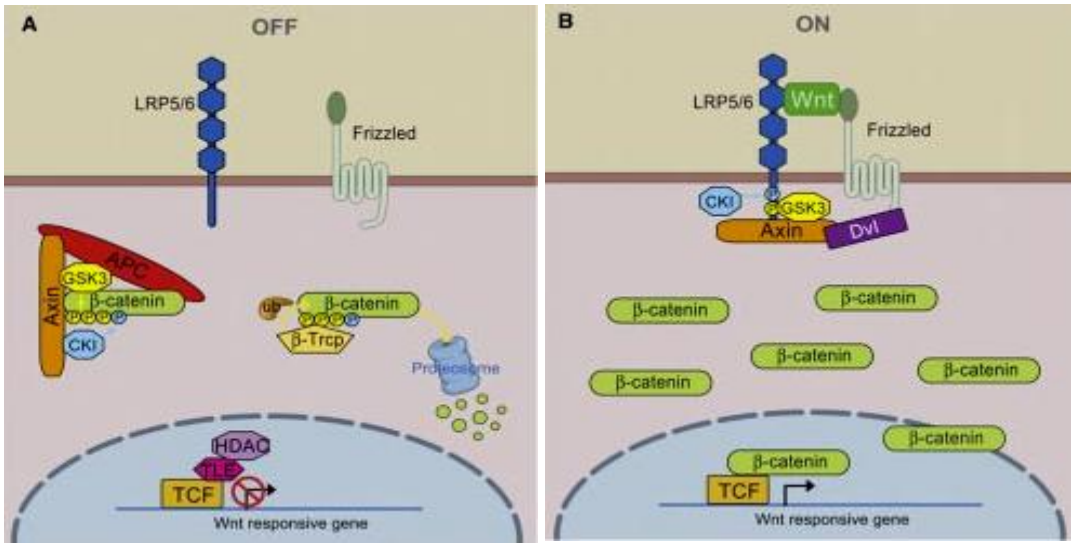

Figure 3. Overview of canonical Wnt signaling. (**A**) Without a Wnt signal, β-catenin is degraded and Wnt target genes are repressed by TCF-TLE/Groucho. (**B**) In the presence of Wnt ligand β-catenin accumulates in the nucleus, where it serves as a co-activator of TCF, leading to transcription of Wnt target genes. APC, adenomatosis polyposis coli; β-Trcp, β-transducin repeat containing protein; CKI, casein kinase; Dvl, Dihevelled; GSK3, glycogen synthase kinase 3β; HDAC, histone deacetylase; LRP5/6, low-density-lipoprotein-related protein 5/6; TCF, transcription factor; TLE, repressor. Adapted from MacDonald B.T. *et al*. (2009). (31)

Without a Wnt signal, as shown in figure 3A, the levels of cytoplasmic β-catenin are kept low due to its degradation by the destruction complex. This destruction complex consists of axin, adenomatosis polyposis coli (APC), protein phosphatase 2A (PP2A), glycogen synthase kinase 3β (GSK-3β) and casein kinase 1α (CK1α). (29)
CK1α and GSK-3β are capable to phosphorylate β-catenin, making β-catenin recognizable to the E3 ubiquitin ligase β-transducin repeat containing protein (β-TrCP). This protein ubiquitinates β-catenin, thereby marking it for proteosomal degradation. (27)(28) As a result, the cytoplasmic levels of β-catenin are kept low, leading to a repressor state of the transcription factor/lymphoid enhancer-binding factor (TCF/LEF), due to the binding of transcriptional repressors, such as p300, C-terminal binding protein (CtBP) and groucho4 .

Binding of Wnt to the Frizzled and LRP5/6 receptor complex on the cell surface leads to two events, 1) the displacement of axin from the destruction complex to the phosphorylated tail of LRP6 and 2) the activation of DVL (Fig. 3B). The activated DVL inhibits GSK-3β, thereby blocking the GSK-3β mediated phosphorylation of β-catenin and preventing the degradation of β-catenin. As a result, stabilized β-catenin accumulates in the cytoplasm. Since β-catenin can only exert its function in the nucleus, it moves into the nucleus by facilitated transport via importins. (32) In the nucleus β-catenin binds to the co-transcription factors TCF/LEF. (25)(29) In the presence of high concentrations of β-catenin the repressors are displaced and gene transcription is stimulated. Several genes are activated through this β-catenin driven transcription, making the canonical Wnt pathway an important controller in the regulation of several cellular mechanisms, in both (embryonic) development and oncogenesis. (33) For example, via gene transcription of CyclinD1 and cMYC, the Wnt pathway regulates cell proliferation and cell survival. (32)(34)(35) The canonical Wnt pathway also plays an important role in cell migration. Wnt-induced expression of SLUG drives EMT, since SLUG represses E-cadherin expression. This reduced E-cadherin expression makes the cells less connected to each other and thus more motile. (36)

1.3.3 The non-canonical pathway

Wnt can also stimulate some pathways independent of β-catenin. There are three non-canonical pathways described, and all of them have Calcium (Ca^{2+}) as a second messenger: 1) the Planar Cell Polarity (PCP) pathway, 2) the Wnt/G protein pathway and 3) the Wnt/Ca^{2+} pathway. These pathways will be shortly described below. (29)

1.3.3.1 The Wnt/Ca^{2+}pathway

As shown in figure 4A, binding of Wnt to Frizzled receptors leads to an increase of intracellular Ca^{2+} and the activation of Ca^{2+}/calmodulin-dependent protein kinase II (CAMKII) and protein kinase C (PKC). As a final result, nuclear factors are activated and gene transcription is turned on. It has been shown that this pathway can interact with the canonical Wnt pathway. For example, CAMKII and PKC are able to phosphorylate β-catenin, thereby serving as negative regulatory components of the canonical Wnt pathway. (26)(32)(37)

1.3.3.2 The Wnt/G protein pathway

Because the Frizzled receptor has seven transmembrane domains, like G-protein coupled receptors, it has been thought that Frizzled receptors can signal via heterotrimeric guanosine triphosphate (GTP) binding proteins (G proteins). (32)

As displayed in figure 4B, signaling via G proteins leads usually to activation of phosphatidylinositol signaling and increased activity of cyclic guanosine monophosphate (cGMP)-selective phosphodiesterases (PDEs), resulting in the transcription of target genes. The main function of this pathway is the regulation of cell morphogenetic movements and adherence. (37)(38)

1.3.3.3 The PCP pathway

Figure 4C demonstrates the PCP pathway. After binding of a Wnt protein to the Frizzled receptor, DVL1 is recruited to the plasma membrane. DVL1 activates small GTPases, such as Rho A and Cdc 42. These GTPases activate Rho-associated Kinase (ROCK) and c-jun-N-terminal kinase (JNK), leading to the transcription of target genes.
Regulation of cell movements and adherence is also the main function of this pathway. (37)(39)

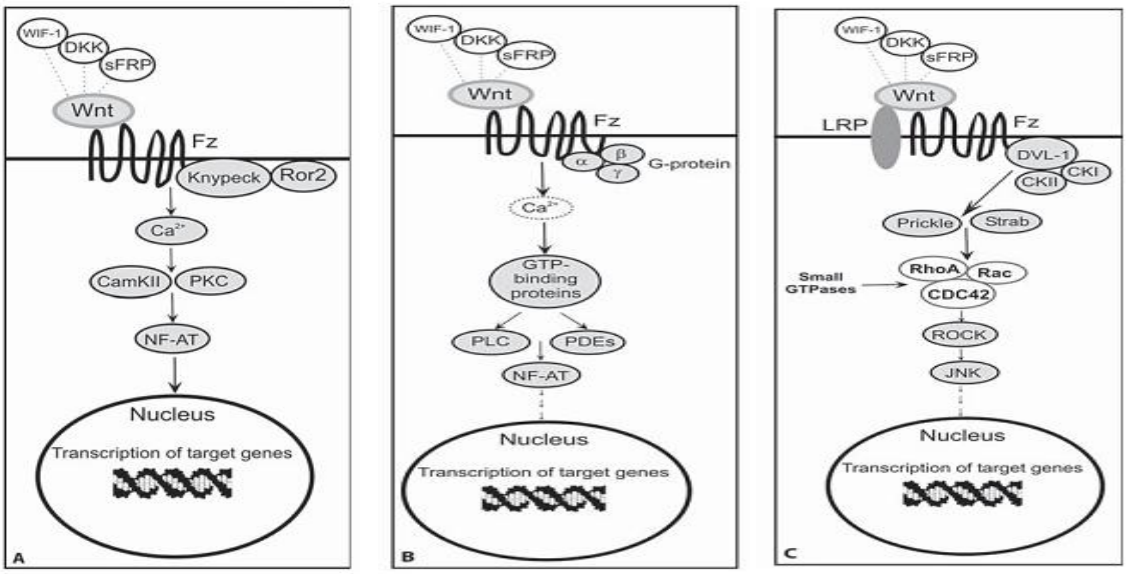

Figure 4. Overview of non-canonical Wnt signaling. (**A**) Wnt/Ca^{2+}pathway, (**B**) Wnt/G protein pathway and (**C**) PCP pathway. Ca^{2+}, calcium; CamKII, Ca^{2+}/calmodulin dependent protein kinase II; CDC42, cell division control protein 42 homolog; DKK, Dickkopf; Fz, Frizzled receptor; GTP, guanosinetrifosfaat; JNK, c-Jun N-terminal kinase; NF-AT, nuclear factor of activated T-cells; PDEs, phosphodiesterases; PLC, phospholipase C; PKC, protein kinase C; Rac, Ras-related C3 botulinum toxin substrate; RhoA, Ras homolog gene family member A; ROCK, Rho-associated kinase; Ror2, receptor tyrosine kinase-like orphan receptor 2; sFRP, secreted frizzled-related protein. Adapted from Turashvili G. *et al.* (2006). (37)

1.3.4 Wnt pathway and the interaction with other pathways

The canonical Wnt pathway is often deregulated in breast cancers. (35) As earlier mentioned, the Wnt pathway is crucial for cell migration, proliferation and survival. So it is imaginable that deregulation of this pathway can have multiple consequences. (40) There are also interactions of the canonical pathway with other pathways described, making the pathway an even more complex pathway.

1.3.4.1 The interaction with the mTOR pathway

In veterinary medicine, surgical excision is the most common therapy for fighting against mammary tumors. However, in human medicine hormonal therapies are also often used. Unfortunately, most tumors become resistant to these hormonal therapies and therefore disease recurrence often occurs. This resistance is linked to hyper activation of the phosphatidylinositol 3-kinase (PI3-K)/mammalian target of rapamycin (mTOR) pathway. (41)(42)

The mTOR pathway is frequently upregulated in breast cancer. The pathway is stimulated by activation of membrane receptor tyrosine kinases (RTK), including the four human epidermal growth factor (EGF) receptors (EGFR/HER1, HER2, HER3 and HER4), and insulin-like growth factor receptor (IGF1-R). Especially HER2-containing dimers strongly activate the mTOR pathway. (43)(44)

After activation of the RTK, PI3K is activated leading to the phosphorylation of phosphatidylinositol 4,5 bisphosphate (PIP_2) to phosphatidylinositol 3,4,4-triphosphate (PIP_3), as shown in figure 5. PIP_3 is an important transducer of signals to downstream components, thereby activating them. Also Protein kinase B (AKT) is phosphorylated and activated by PIP_3, making AKT able to phosphorylate other targets, including the mTOR complex. The mTOR complex is a key regulator of cell growth, proliferation, survival and protein synthesis. Phosphatase and tensin homolog (PTEN) antagonizes PI3K activity, by dephosphorylating PIP_3. PTEN is therefore an important tumor suppressor. However, loss of PTEN is often found in breast cancer. (45-48)

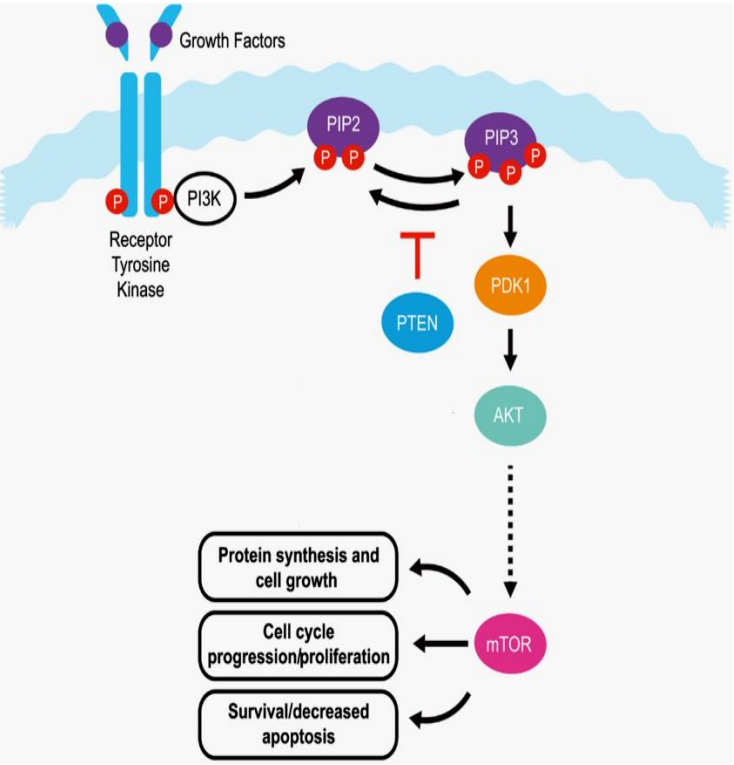

Figure 5. Overview of the PI3K/AKT/mTOR pathway. Binding of growth factors to the receptor tyrosine kinase activates PI3K. Activated PI3K converts PIP2 to PIP3, which leads to phosphoryation of Akt. Activated Akt activates mTOR, with cell growth, cell proliferation and cell survival as result. Akt, protein kinase B; mTOR, mammalian target of rapamycin; PDK1, pyruvate dehydrogenase kinase 1; PI3K, phosphatidylinositol 3-kinase; PIP2, phosphatidylinositol 4,5 biphosphate; PIP3, phosphatidylinositol 3,4,4-triphosphate; PTEN, phosphatase and tensin homolog. Adapted from Phin S. *et al.* (2013). (48)

To restore the sensitivity to hormonal therapies caused by the hyperactivation of the mTOR pathway, mTOR inhibitors are used. For example, additional therapies with the mTOR inhibitor Everolimus are recently started in human patients with estrogen receptor positive breast cancer. (49) Studies have shown that hormonal therapy combined with Everolimus leads to an increase in survival duration. (50)(51)

However, in vitro experiments have shown some side effects of mTOR inhibitors. Canine mammary tumor cell lines with low and high canonical Wnt activity were treated with several inhibitors to test the effect on Wnt activity. The experiment showed that the mTOR inhibitor Everolimus and the dual PI3K and mTOR inhibitor BEZ235 enhance the Wnt activity of the cell lines with already upregulated canonical Wnt activity. The same experiment showed that the addition of the SRC inhibitor SRC-I1 inhibits the Wnt activity of cells with high basal canonical Wnt activity.
These findings suggest that there could be a connection between the pathways, and that SRC could be the connecting factor between both pathways.
Furthermore, the cell lines were compared to each other to discover possible causes of the high canonical Wnt activity of some cell lines. Because mutations in the components of the destruction complex often lead to over activation of the canonical Wnt pathway, the cell lines were screened on

possible mutations. However, mutational analysis of coding sequences of the components of the destruction complex showed no mutations which were specific to the cell lines with high canonical Wnt activity. Gene expression analysis revealed that high Wnt activity is accompanied by higher expression of HER2, HER3 and LEF1, and by a loss of PTEN. A study of Gracanin *et al*. already showed that the overexpression of LEF1 indeed contributes to high canonical Wnt activity, but the study also showed that the high expression of LEF1 does not affect the expression and stabilization of β-catenin. (52)(53)

2. Aim and outline of this study

This Honours Programme focused on two different components of the canonical Wnt pathway:

1) The interaction between the Wnt pathway and the mTOR pathway.

This part of the research, which is described in chapter 3, had as prominent goal to find out how these pathways are connected to each other.
Previous research showed that the SRC inhibitor SRC-I1 inhibit the Wnt activity of canine mammary cell lines with upregulated canonical Wnt activity, suggesting that SRC influences the canonical Wnt pathway. In literature, interactions between SRC and the EGF receptors, which have the mTOR pathway as downstream pathway, are described. Therefore, our hypothesis was that SRC is the connecting factor between both pathways.

2) The overexpression of HER2 and HER3 in relation to the high basal canonical Wnt activity of certain canine mammary tumor cell lines.

The second part of this research year, which is described in chapter 4, had as prominent goal to find out if the overexpression of HER2 and HER3 contributes to the high basal canonical Wnt activity of three certain canine mammary tumor cell lines. These cell lines show a factor three upregulated expression of HER2 and even a factor 45 upregulated HER3 expression.
As mentioned in the general introduction, previous research showed that mutations in the β-catenin destruction complex are not the cause of the increased basal canonical Wnt activity in these three canine mammary cell lines. Also the overexpression of LEF1 does not explain the highly basal activated canonical Wnt pathway. Therefore, it is reliable that other factors contribute to the high basal canonical Wnt activity. In search for an explanation of the highly basal activated canonical Wnt pathway in these three canine mammary cell lines, we found it a logical next step to focus on HER2 and HER3, to obtain their possible contributing role in the canonical Wnt pathway.

The studies performed in this Honours Programme are embedded in the fundamental research group *Tissue Repair* of the Faculty of Veterinary Medicine, Utrecht University. Furthermore, this study is also embedded in the PhD Programme of Ing. Elpetra Timmermans-Sprang.

3. The interaction between the canonical Wnt pathway and the mTOR pathway

3.1 Abstract

Background: Previous research showed that SRC can influence canonical Wnt activity. According to literature, SRC can interact with EGF receptors, which are upregulated in the canine mammary tumor cell lines with high basal canonical Wnt activity. Taken these findings together, there is a strong indication that an interaction between the mTOR pathway (downstream pathway of the EGF receptors) and the canonical Wnt pathway exists, possibly via SRC and kinase pathways related to SRC.

Objectives: The aim of this part of the study was to identify how both pathways are connected to each other.

Methods: Two cell lines were used; CMT-U27 (cell line with high basal canonical Wnt activity) and CIPm (cell line with low Wnt activity). The cell lines were treated with compounds related to SRC, and effects were measured on cell viability (MTT assay), canonical Wnt activity (TCF-reporter assay) and cell migration (scratch assay).

Results: The cell viability assay showed that CMT-U27 cells are 13 times more sensitive to inhibition of Aurora kinase A (Aurora A inhibitor 1) and about 11 times more sensitive to inhibition of both Aurora kinase A and B (Barasertib). The TOP/FOP assay showed that the compounds Dasatinib (targets Abl and SRC), OSI-906 (targets IGF-1R) and PP2 (targets FYN and LCK) significantly inhibit the canonical Wnt activity of the CMT-U27 cell line. A significant decreased migration rate was found in the CMT-U27 cells treated with PP2 and SRC-I1.

Conclusions: No direct relation exists between the viability results as measured by MTT and the effects on canonical Wnt signaling. Based on the results of the TOP/FOP assay and the scratch assay it is concluded that SRC plays a prominent role in connecting the mTOR pathway and the canonical Wnt pathway.

3.2 Introduction

The SRC family of protein kinases (SFKs) belongs to the family of non-receptor tyrosine kinases. SFKs consist of nine members: BLK, FGR, FYN, HCK, LCK, LYN, SRC, YES and YRK, among which SRC is a major player in breast cancer. (54-56)

The activity of SFKs is regulated by intramolecular interactions. Interactions between the SH2 domain and the C-terminal tail and interactions between the SH3 domain and a polyproline-type helix in the SH2-kinase linker region lead to the inactive state of SFKs. As a result, tyrosine kinase (TK) activity is suppressed. Binding of ligands to the SH2 and SH3 domains interrupt these auto inhibitory interactions, thereby promoting TK activity. (57)

The most well-studied function of SRC is the interaction with RTKs at the cell membrane. These interactions occur via the SH2 and SH3 domains of SRC, thereby activating the SFKs. It is known that SRC interacts with several RTKs, such as epidermal growth factor receptor (EGFR), HER2, platelet-derived growth factor receptor (PDGFR), insulin-like growth factor-1 (IGF-1R) and c-Met/hepatocyte growth factor receptor (HGFR). These interactions make SRC an important transducer of signals to downstream effectors. (58)

Previous studies have shown that the SRC inhibitor SRC-I1 inhibits canonical Wnt activity, measured by TCF-reporter assay. Gene expression analysis with qPCR also revealed that SRC-I1 downregulates

genes involved in the canonical Wnt pathway. So, these results indicate that SRC influences canonical Wnt activation.
As already mentioned in the general introduction, the cell lines with high canonical Wnt activity show an upregulation of the EGF receptors. As mentioned above, SRC can interact with the EGF receptors. (59) Taken these findings together, our hypothesis is that SRC is the connecting factor between the downstream pathway of the EGF receptors (the mTOR pathway) and the canonical Wnt pathway.

But, results obtained from earlier performed experiments show that SRC-I1 only affects cell proliferation and Wnt activity when the inhibitor is used at a relatively high concentration, namely 20 µM. The concentrations which induce 50% cell death (the IC50-values) are (mostly) known for all chemicals. According to J. Bain *et al*. the IC50-value of SRC-I1 would be around 0.18 µM, so far below the concentration which affects cell proliferation and Wnt activity in our cell lines. (60)(61) The remaining question is why the inhibitor only affects cell proliferation and Wnt activity when used at a concentration far above the IC50-value. One explanation could be that canine SRC is insensitive to inhibition, so that inhibition only occurs when using high concentrations. Another explanation could be that there is cross reactivity between SRC and some other kinase pathway(s). The effect on cell proliferation and Wnt activity could then also be caused by the inhibition of another kinase and that will make SRC no longer the main player. According to literature SRC can interact with several pathways. (58)(62) We therefore studied the cell viability, the basal Wnt activity and the effect on cell migration of a panel of specific inhibitors related to SRC-I1 on two canine mammary cell lines.

3.2.3 Outline of the study

To test if other kinases could be involved in both pathways, cell viability (MTT) assay was performed firstly. Several inhibitors with different targeting pathways which all could possibly interact with SRC were tested. These inhibitors were added to two different cell lines to test if there are differences in sensitivity to inhibition between cells with high basal Wnt activity (CMT-U27) and cells with low basal Wnt activity (CIPm).

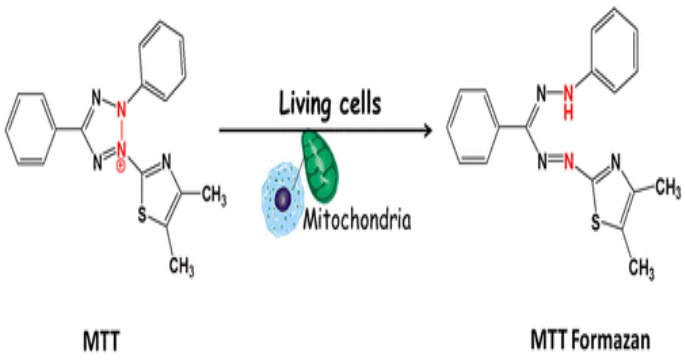

Figure 6. The mechanism behind cell viability (MTT) assay. The assay distinguishes live from dead cells, since live cells have active mitochnodria which possess an enzyme system which cleavages the tetrazolium ring of yellow MTT leading to the formation of purple formazan. Adapted from Mao Z. *et al.* (2013). (63)

The MTT assay is a cell viability assay which distinguishes live from dead cells. MTT [3- (4,5-Dimethyl-2-thiazolyl)-2,5-diphenyl-2H-tetrazolium bromide] is a yellow dye which transposes into a purple dye when reduced by living cells. Active mitochondria possess an enzyme system which cleavages the tetrazolium ring of MTT leading to the formation of purple formazan (Fig. 6). Only living cells are able to induce this change in color, since dead cells do not have active mitochondria. The amount of formazan detected by a spectrophotometer is then indicative for the number of living cells. (63)

Afterwards, TCF-reporter assay, also known as TOP/FOP assay, was performed to test the effect of the eight compounds on the canonical Wnt activity.

TCF-reporter assay is measured with a Dual-Luciferase Reporter (DLR) Assay System. The assay is based on the presence of nucleocytoplasmic β-catenin, considered as a hallmark of activity of the canonical Wnt pathway. In this assay firefly (*Photinus pyralis*) luciferase and Renilla (*Renilla reniformis*) luciferase are measured serially in a sample. Cells are transfected with either a TOPflash (TOP), containing wild-type TCF/LEF-1 binding sites, or a FOPflash plasmid (FOP), containing mutated TCF/LEF-1 binding sites and with a β-Actin-promoter-Renilla construct. These plasmids are linked to a promoter that drives luciferase gene expression. This firefly luciferase signal is measured first by adding Luciferase Assay Reagent. After that, the Stop and Glo Reagent is added to initiate the Renilla luciferase signal, which serves as a control reporter activity to measure transfection efficiency. (64)

Thereafter, a scratch assay was performed to test the effects of inhibitors, which stimulate the canonical Wnt pathway, and inhibitors which inhibit Wnt activity, on the migration capacities of the two cell lines. Because stimulation of the canonical Wnt pathway leads to EMT (36), we wanted to test *in vitro* if the migration rate of CMT-U27 cells increases after incubation with Wnt stimulators. In addition, it was tested if inhibition of the canonical Wnt pathway results in a decreased migration rate of CMT-U27 cells.

A scratch assay is a relatively simple and inexpensive migration assay. The principle of a scratch assay is, when the cells have reached a confluent monolayer, to create an area without cells (the ‘’wound’’) giving the cells the opportunity to migrate. When taking pictures of the wound at certain time points, the migration rate can be calculated when comparing the wound distances of a certain time point to the ‘original’ wound distance immediately after scratching. So, the percentage of wound closure is indicative for the migration capacities of cells. (65)

3.3 Materials and methods

3.3.1 Cell culture

Canine mammary tumor cell lines used in this study were CMT-U27 and CIPm. The cell lines were generous gifts of Prof. Dr. Hellmen (SLU, Uppsala, Sweden) and Prof. Dr. Sasaki (Laboratory of Veterinary Surgery, University of Tokyo, Japan). The CMT-U27 cell line was derived from a primary canine mammary carcinoma. This cell line contains a highly upregulated canonical Wnt pathway. The CIPm cell line has its origin from a metastasis to a regional lymph node of a canine mammary carcinoma. This cell line contains low Wnt activity. Both cell lines were cultured in DMEM/F12 (#11320-074, Gibco, Life technologies, Bleiswijk, The Netherlands), supplemented with 10% Fetal Calf Serum (FCS) (#10270-106, Gibco, Life technologies) and 1% antibiotics (Penicillin and Streptomycin) (#15140-122, Gibco, Life technologies). All cell culture handlings were performed in a vertical flow cabinet. Both cell lines were passaged twice a week. To detach the cells 2 ml TrypLE Express (#12604-013, Gibco, Life technologies) was added to the cells. After detaching, the sterile T75 culture flasks (#658175, Greiner Bio-One, Kremsmünster, Austria) with the desirable amount of cells were placed in an Innova CO-170 incubator (New Brunswick Scientific, Edison, New Jersey, USA) at 37°C and 5% CO_2 to let the cells attach and grow.

Because of differences in cell morphology between the CMT-U27 and the CIPm cell line, different seeding concentrations were used during cell culture assays. CMT-U27 cells are small partially rounded cells, whereas CIPm cells show a stretched out spindle-like structure. Therefore, CMT-U27 cells were seeded in higher concentrations than CIPm cells to guarantee the same cell confluence of both cell lines at the start of an experiment.

3.3.2 Cell viability

Eight inhibitors with different susceptibilities to different kinase pathways were tested (Table 1). The inhibitors were dissolved in Dimethyl Sulfoxide (DMSO) (#1029500500, Merck Millipore, Billerica, MA, USA) to a final stock concentration of 10 mM.

Table 1. Overview of compounds used for cell viability (MTT) assay. Eight compounds with different targets which possibly interact with SRC were added to CMT-U27 cell line and CIPm cell line to test the involvement of other kinases in the mTOR pathway and the canonical Wnt pathway.

Name	Target	IC50-value according to manufacturer
Afatinib (#S1011, Selleckchem, Munich, Germany)	EGFR and HER2	0.5 nM and 14 nM
Aurora A Inhibitor I (#S1451, Selleckchem)	Aurora A, B and C	3.4 nM, 3.4 µM and 0.432 µM
AZD1480 (#S2162, Selleckchem)	JAK2	0.26 nM
AZD7762 (#S1532, Selleckchem)	CHK1 and CHK2	5 nM and <10 nM
Barasertib (#S1147, Selleckchem)	Aurora B and A	0.37 nM and 37 nM
Dasatinib (#S1021, Selleckchem)	Abl and SRC	0.6 nM and 0.8 nM
OSI-906 (#S1091, Selleckchem)	IGF-1R	35 nM
PP2 (#S7008, Selleckchem)	LCK and FYN	4 nM and 5 nM

CMT-U27 cells were seeded in 96-wells Primaria plates (#353872, Corning, New York, USA) at a density of 15.000 cells/100 µl DMEM/F12 with 10% FCS and without antibiotics, while CIPm cells were seeded at a concentration of 10.000 cells/100 µl. After 24 hours incubation in the Innova CO-170 incubator 10 µl of the inhibitors was added to the cells. The inhibitors were added in a concentration range from 1 nM to 1mM. To exclude the possibility that effects are caused by DMSO instead of the inhibitors, two controls were used. Cells treated with only medium and cells treated with 0.2% DMSO were compared to each other, to determine the effect of 0.2% DMSO on cell viability, since the final concentration of DMSO in which the inhibitors are dissolved is 0.2% in each well. Per condition an average of 6 wells was used for calculation and the MTT assay was performed twice. So, the total amount of wells per condition was 12 (n=12).

3-[4,5-dimethylthiazol-2-yl] 2,5-diphenyltetrazolium bromide (MTT) (#M5655 SIGMA, Sigma-Aldrich, Zwijndrecht, the Netherlands) was weighed and dissolved in Hank's Balanced Salt Solution (1x)(# 14025-050, Gibco, Life technologies) to a final concentration of 5 mg/ml. Afterwards, this solution was filtered to a 22 µm syringe filter (#SLGV033RS, Merck Millipore) to sterilize the solution.
48 hours after the addition of the inhibitors, 20 µl MTT was added to the cells. Then, the 96-wells plates were incubated for two hours at 37 °C and 5% CO_2. After incubation the plates were decanted and 100 µl DMSO was added to each well. The plates returned into the incubator for 30 minutes. Thereafter, the absorbance was measured at 595 nm using an Anthos plate reader (DTX 880 Multimode detector spectrophotometer, Beckman Coulter, using the Software for Anthos Multimode Detectors, version 2.0.0.13) The data obtained from the Anthos plate reader were converted to an Excel-file for further analysis and calculations. The absorbance of the control was set to 100% and the percentages of cell viability of the samples were calculated relative to the control with the following formula: (absorbance sample/absorbance control) *100%. The software Sigmaplot12.5 was used to create graphs and to calculate the IC50-values.

3.3.3 TCF-reporter assay

The TCF-reporter assay is based on the presence of nucleocytoplasmic β-catenin, considered as a hallmark of activity of the canonical Wnt pathway. In the assay cells are transfected with either a TOP, containing wild-type TCF/LEF-1 binding sites, or a FOP containing mutated TCF/LEF-1 binding sites. Cells are also transfected with a β-Actin-promoter-Renilla construct to test transfection efficiency.

CMT-U27 cells were seeded in 24-wells Primaria plates (#353847, Corning) at a concentration of 100.000 cells/ml DMEM/F12 with 10% FCS without antibiotics. CIPm cells were not seeded, because these cells have barely Wnt activity and previous TOP/FOP assays had already shown that several inhibitors do not affect this low Wnt activity.

After 24 hours, when the cells had reached a confluence of approximately 80%, the cells were washed once with 1 ml Hanks. After that, 400 µl DMEM/F12 without FCS and antibiotics was added to the wells. Then the Lipofectamine 2000 (#11668019, Invitrogen, Life technologies) and TOP and FOP mixes were made. After 5 minutes incubation time on room temperature the same amount of lipofectamine was added to the TOP and the FOP mix. These mixes were then incubated for 20 minutes on room temperature. In total: the cells were transfected with 100 µl DMEM/F12 containing 3 µl Lipofectamine 2000, 800 ng TOP or 800 ng FOP (gift from Prof. Dr. Hans Clevers, Hubrecht Institute, The Netherlands) and 0.5 ng human β-actin-promoter-renilla construct. (66)

After 5 hours incubation at 37 °C and 5% CO_2 the transfection was stopped by adding 500 µl DMEM/F12 with 20% FCS to the wells. Then, 100 µl of the IC50-value of the inhibitors, obtained from the MTT assay, was added to the wells. Again, cells treated with only medium and 0.2% DMSO served as control groups. Per condition 4 wells were used, and the experiment was performed three times (n=12).

48 hours after addition of the inhibitors, the medium was sucked off and the cells were washed once with 1 ml Hanks. Next, 100 µl 5 times diluted Promega lysis buffer (#E1910, Promega, Leiden, The Netherlands) was added and the plates were agitated for 15 minutes. After that, the plates were put in the -70 °C freezer for 30 minutes.
After thawing, 100 µl of the lysated cell suspension was pipetted in a V-shape 96-wells plate (#651191, Greiner Bio-one). This plate was centrifuged at 3000 rpm for 15 minutes. After centrifuging, 20 µl of the supernatant was pipetted in a white 96-wells plate with a flat bottom (#3600, Corning)
Then, the TOP, FOP and Renilla activities were measured in a luminometer (LUMIstar Galaxy luminometer, BMG Labtech GmbH, Ortenberg, Germany) by adding 36 µl Luciferase and 36 µl Stop and Glo (#E1910, Promega).

Both TOP and FOP data are corrected for transfection efficiency, by dividing the data by the Renilla data (Corrected TOP = TOP/REN and Corrected FOP= FOP/REN). Then, the TOP to FOP ratio is calculated by the following formula: Corrected TOP/Corrected FOP.

3.3.4 Scratch assay

Firstly, an experiment was performed to determine the optimal seeding densities of the cells. Before starting with scratching, a monolayer of cells is required. Therefore, it was tested what the optimal seeding concentrations are to obtain a confluent monolayer of cells 24 hours after plating the cells. This experiment showed that CMT-U27 cells formed a monolayer after 24 hours when plating the cells at a density of 1x10^6 cells/3 ml DMEM/F12 with 10% FCS without antibiotics and CIPm at a density of 500.000 cells/3ml.

So, 1x10^6 CMT-U27 cells and 500.000 CIPm cells were seeded in six-well plates (#353846, Corning). After 24 hours, the cell monolayer was scraped with a 1-200 µl pipet tip (#4823, Corning) to create a straight as possible line.
Then, medium was removed and the cells were washed twice with 1 mL Hank's Balanced Salt solution (# 14025-050, Gibco) to remove detached cells and debris.
Thereafter, inhibitors were added to the cells. The mTOR inhibitor Everolimus (#S1120, Selleckchem) and the dual PI3K/mTOR inhibitor BEZ235 (#S1009, Selleckchem) were added in a concentration of 100 nM and 50 nM, respectively. Of the SRC inhibitors 20 µM SRC-I1 (#BML-EI398, Enzo) and 10 µM PP2 (#S7008, Selleckchem) was added to the cells. PP2 was used as a positive control, since other reports already showed that PP2 decreases migration rates of breast cancer cell lines, caused by an inhibition of transcription factors which are involved in EMT. (67)
Cells treated with 0.2% DMSO served as control to exclude the opportunity that the effects are caused by DMSO, since the inhibitors are dissolved in a final concentration of 0.2% DMSO.

In each experiment three areas were measured in each well and at least two wells per condition were used (n≥6). Reference points were made on the outer bottom of the wells to assure the same

areas during the image acquisition. Otherwise, comparing the pictures is not really reliable. Images from cells migrating into the scratch were captured after 0, 24 and 48 hours with an Olympus microscope (Olympus, Tokyo, Japan). All pictures were taken when using the 4x objectives. The images were then analyzed with the computing software ImageJ analysis version 1.4.7.
Finally, the migration rate was calculated as percentage of scratch closure with the following formula: a-b/a, where a is the distance of the wound at t=0, and b is the distance of the wound at t=24 or t=48.

3.3.5 Statistical analysis

Statistical analysis was conducted using IBM SPSS Statistics version 22 software (SPSS Benelux, Gorinchem, The Netherlands). Data were normally distributed, so the one-way ANOVA and the post-hoc Bonferroni tests were applied. When compared to the DMSO control group, a P-value <0.05 was regarded as significant, indicated with an asterisk (*) in the figure.

3.4 Results

3.4.1 Cell viability

No differences were found between the absorbance data of CMT-U27 cells and CIPm cells in the two control conditions (0.2% DMSO versus medium). From this, we concluded that 0.2% DMSO does not affect the cell viability of these cell lines and therefore we assumed that changes in cell viability are only caused by the inhibitors.

Below, the IC50-graphs created with Sigmaplot12.5 are shown. On the Y-axis the absorbance is displayed and on the X-axis the concentrations in a logarithmic scale can be read out (Fig. 7).

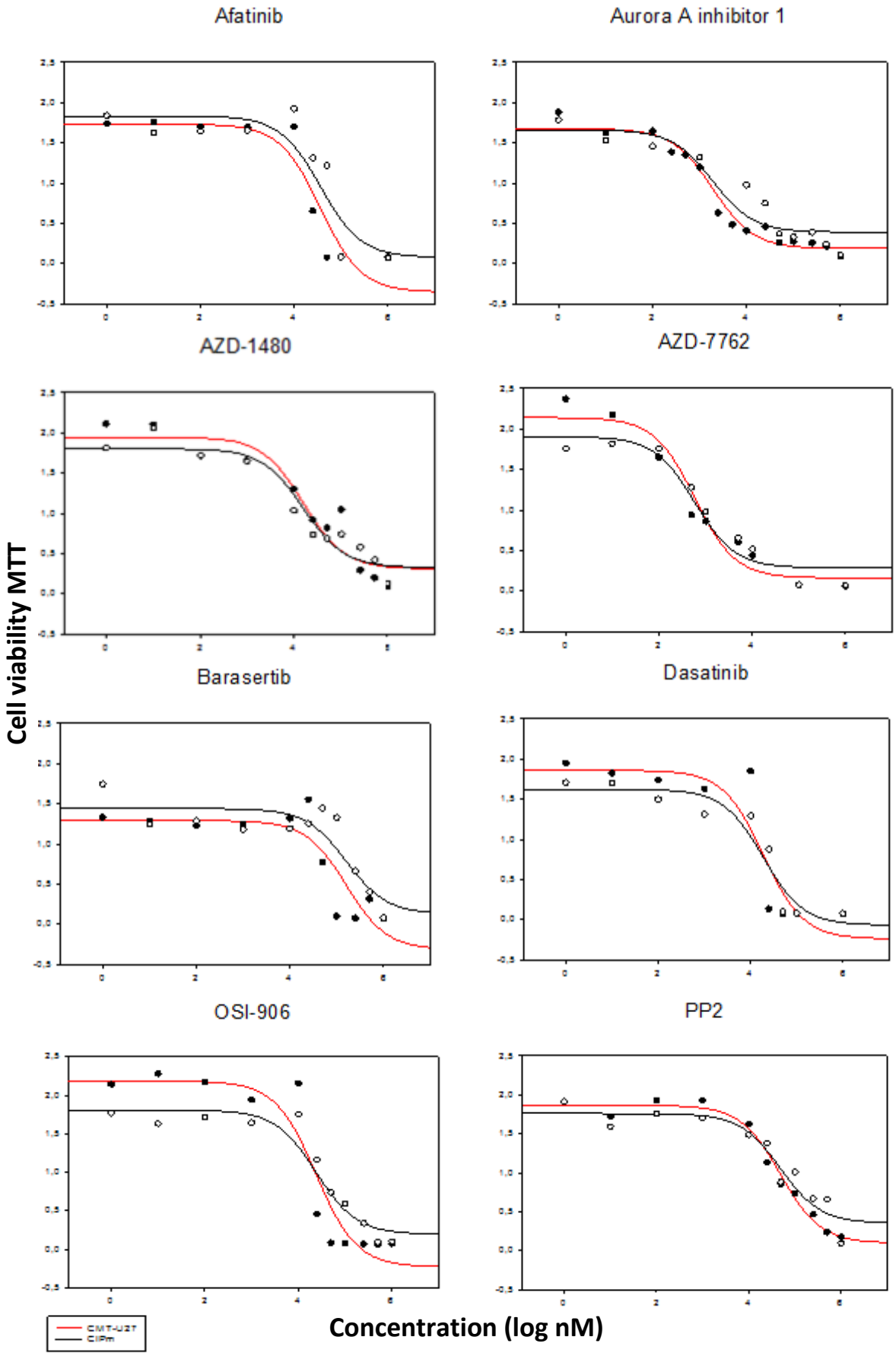

Figure 7. IC50 curves. CMT-U27 (high TOP/FOP ratio) and CIPm cells (low TOP/FOP ratio) were grown for 48 hours with the eight inhibitors in increasing concentrations (1 nM- 1mM). After 48 hours the cell viability was measured with a MTT assay. Results are the mean of 12 samples out two independent experiments (n=12). IC50-values were calculated with Sigmaplot software (version 12.5).

The obtained IC50-values are summarized in the table below:

Table 2. Overview of obtained IC50-values of cell viability assay of CMT-U27 and CIPm cell line.

Name	CMT-U27	CIPm
Afatinib	22 µM	69 µM
Aurora A inhibitor 1	1 µM	13 µM
AZD1480	28 µM	9 µM
AZD7762	301 nM	1 µM
Barasertib	77 µM	822 µM
Dasatinib	17 µM	23 µM
OSI-906	18 µM	54 µM
PP2	41 µM	70 µM

The IC50-values show that CMT-U27 cells are, in general, more sensitive to inhibition, except for inhibition of JAK2 (AZD1480). Of the eight compounds, CMT-U27 cells are most sensitive for inhibition of CHK1 and CHK2 (AZD7762). The sensitivity to inhibition of most targets does not differ a lot between both cell lines. However, CMT-U27 cells showed to be 13 times more sensitive to inhibition of Aurora kinase A (Aurora A inhibitor 1) and about 11 times more sensitive to inhibition of both Aurora kinase A and B (Barasertib) than CIPm cells.

3.4.2 TCF-reporter assay

Firstly, the results showed that the TOP/FOP ratios of the CMT-U27 cells in DMSO control condition and the CMT-U27 cells in medium control condition barely differ from each other, so that effects caused by DMSO can be excluded.

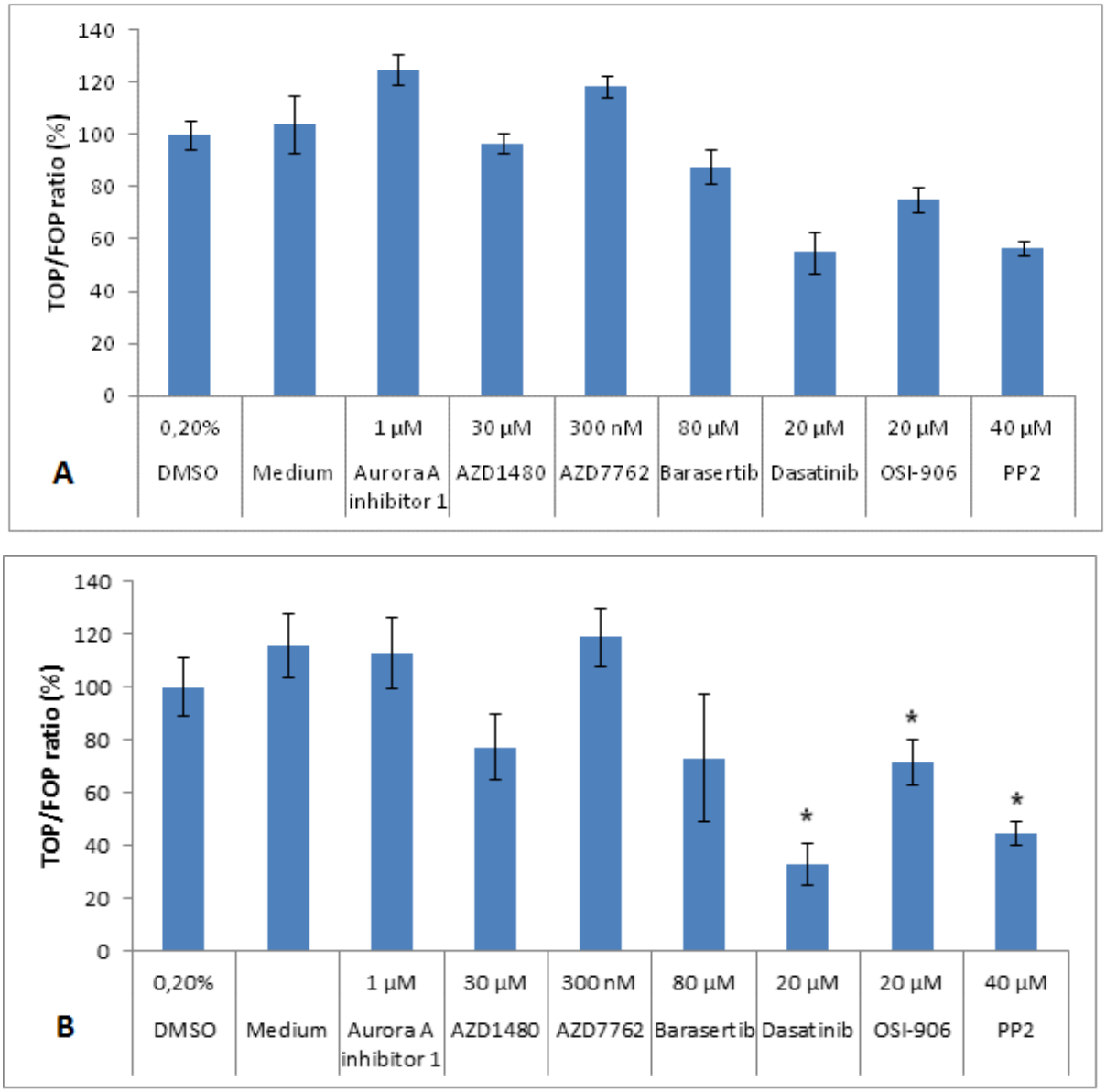

Figure 8. Effects of seven compounds on basal Wnt activity of CMT-U27 cells as measured by the TOP/FOP ratio. The cell line was grown for 48 hours in the presence of Aurora A inhibitor 1 (1 µM), AZD1480 (30µM), AZD7762 (300 nM), Barasertib (80 µM), Dasatinib (20 µM), OSI-906 (20 µM) and PP2 (40 µM). After 48 hours the TOP/FOP ratio was measured with a Dual-Luciferase assay. Results expressed as % of DMSO control (set to 100%) are the mean (±SEM) of 12 samples out three independent experiments (n=12). (**A**) Results are expressed as the TOP/FOP ratio with correction for transfection efficiency. Because of the lack of a stable Renilla signal, the amount of usable results was limited, and therefore no statistics were performed on these data. (**B**) Results are expressed as the TOP/FOP ratio without correction for transfection efficiency. $P<0.05$ is marked as * and indicates a significant difference compared to the DMSO control. Incubation with Dasatinib, OSI-906 and PP2 shows a significant down regulation of the basal Wnt activity in the CMT-U27 cell line.

The effects of seven compounds on canonical Wnt activity of CMT-U27 cells, with correction for transfection efficiency, are shown in figure 8A. The inhibitors AZD1480, Barasertib, Dasatinib, OSI-906 and PP2 showed inhibitory effects on canonical Wnt activity of CMT-U27 cells. Compared to CMT-U27 cells in DMSO control condition, AZD1480, Barasertib, Dasatinib, OSI-906 and PP2 inhibited the canonical Wnt activity with 3%, 12%, 45%, 25% and 44%, respectively. The compounds Aurora A inhibitor 1 and AZD7762 showed stimulatory effects on canonical Wnt activity. Compared to CMT-U27 cells in DMSO control condition, the inhibitors stimulated the Wnt activity with 25% (Aurora A inhibitor 1) and 33% (AZD7762).

The effects of the seven inhibitors on canonical Wnt activity of the CMT-U27 cell line, without correction for transfection efficiency, but with statistical analysis, are shown in figure 8B. Again, the inhibitors AZD1480, Barasertib, Dasatinib, OSI-906 and PP2 showed inhibitory effects on canonical Wnt activity, while the inhibitors Aurora A inhibitor 1 and AZD7762 showed stimulatory effects on canonical Wnt activity. Compared to CMT-U27 cells in DMSO control condition, the inhibitors AZD1480, Barasertib, Dasatinib, OSI-906 and PP2 again inhibited canonical Wnt activity, with 23%, 27%, 67%, 28% and 56%, respectively. Aurora A inhibitor 1 and AZD772 showed stimulatory effects on canonical Wnt activity, with an increase of 13% and 39%, respectively. Of these results, only the administration of Dasatinib, OSI-906 and PP2 resulted in significant altered Wnt activity compared to DMSO control CMT-U27 cells.

3.4.3 Scratch assay

3.4.3.1 Migration of CMT-U27 cell line

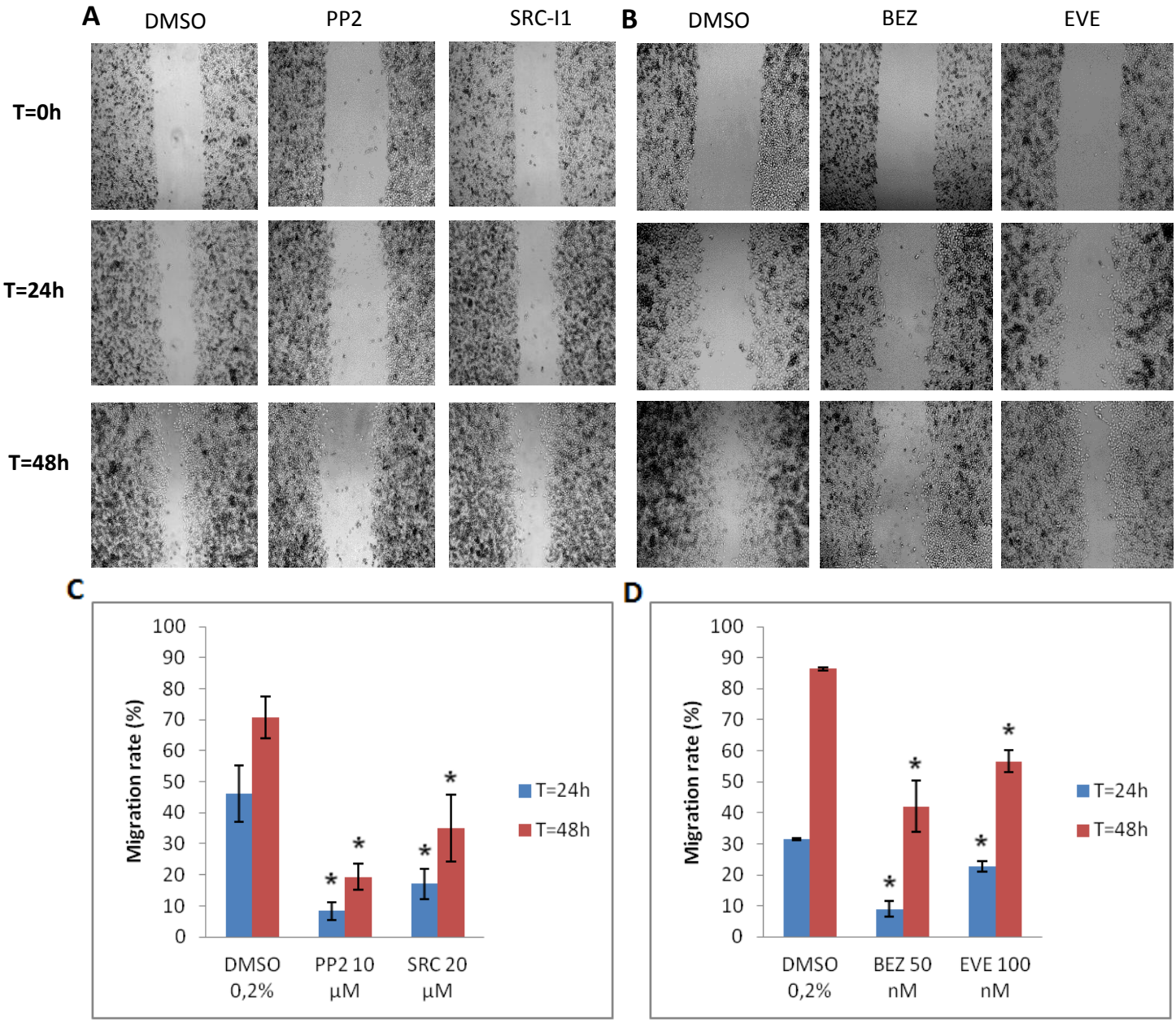

Figure 9. Scratch assay of CMT-U27 cell line (with a high TOP/FOP ratio) in control conditions (0.2% DMSO) and after treatment with two SRC inhibitors and two mTOR inhibitors. Representative images of scratch closure in control condition (0.2% DMSO) and after PP2 (10 µM) and SRC-I1 (20 µM) treatment (**A**) and after BEZ (50 nM) and Everolimus (100 nM) treatment (**B**) in CMT-U27 cell line. Images were taken using lens with 4x magnification and analysed using ImageJ analysis version 1.4.7. Images were taken immediately after scratching (T=0h), and after 24 and 48 hours (T=24h and T=48h). Quantification of migration of CMT-U27 cell line after treatment with SRC inhibitors (**C**) and after treatment with mTOR inhibitors (**D**) are presented as percentages of scratch closure and are calculated as follows: % of scratch closure = a-b/a, where (a) is the distance of the wound at T=0h, and (b) is the distance of the wound at T=24h and T=48h. Results are expressed as the mean (±SEM) of six measurements out two independent experiments (n=6). *P*<0.05 is marked as * and indicates a significant difference compared to the DMSO control.

3.4.3.2 Migration of CIPm cell line

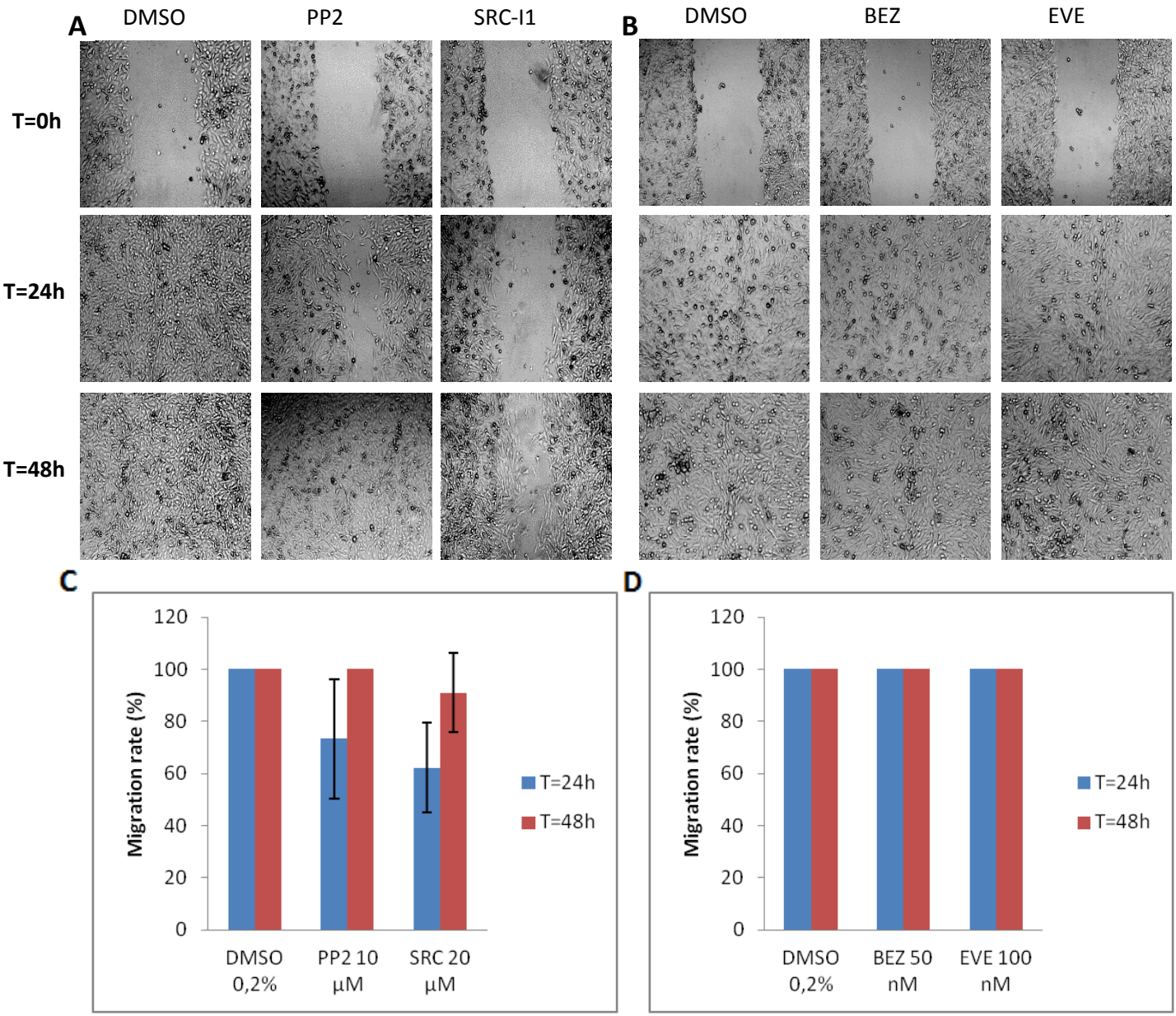

Figure 10. Scratch assay of CIPm cell line (with a low TOP/FOP ratio) in control conditions (0.2% DMSO) and after treatment with two SRC inhibitors and two mTOR inhibitors. Representative images of scratch closure in control condition (0.2% DMSO) and after PP2 (10 µM) and SRC-I1 (20 µM) treatment (**A**), and after BEZ (50 nM) and Everolimus (100 nM) treatment (**B**) in the CIPm cell line. Images were taken using lens with 4x magnification and analysed using ImageJ analysis version 1.4.7. Images were taken immediately after scratching (T=0h), and after 24 and 48 hours (T=24h and T=48h). Quantification of migration of CIPm cell line after treatment with SRC inhibitors (**C**) and after treatment with mTOR inhibitors (**D**) are presented as percentages of scratch closure and are calculated as follows: % of scratch closure = a-b/a, where (a) is the distance of the wound at T=0h, and (b) is the distance of the wound at T=24h and T=48h. Results are expressed as the mean (±SEM) of six measurements out two independent experiments (n=6). No significant differences were found compared to the DMSO control.

As shown in figure 9A and 9C, both SRC inhibitors caused strong inhibitory effect on cancer cell migration in the CMT-U27 cell line. While in DMSO control condition cells showed migration rates of 46% and 70% (after 24 and 48 hours, respectively), after PP2 administration CMT-U27 cells showed migration rates of 8% and 19%, and after SRC-I1 administration migration rates of 17% and 35%. So compared to the DMSO control, PP2 inhibited migration rates of CMT-U27 cells with 38% and 51%, and SCR-I1 with 29% and 35%, at 24 and 48 hours respectively.

Figures 9B and 9D show the migration of CMT-U27 cells after treatment with the dual PI3K/mTOR inhibitor BEZ and with the mTOR inhibitor Everolimus. Both inhibitors significantly inhibited migration rates of CMT-U27 cells when compared to the DMSO control. The CMT-U27 cells treated with BEZ showed migration rates of 9% and 42%, and CMT-U27 cells treated with Everolimus showed migration rates of 22% and 56%, while in control condition CMT-U27 cells had migration rates of 32% and 86%, at 24 and 48 hours respectively. So compared to CMT-U27 cells in DMSO control condition, BEZ administration inhibited the migration rate with 23% and 44%, and Everolimus treatment inhibited with 10% and 30%, at 24 and 48 hours.

As shown in figure 10A and 10C, both SRC inhibitors proved to be inhibitors of cell migration in the CIPm cell line, although not significant compared to CIPm cells in DMSO control condition. While in control condition CIPm cells showed a migration rate of 100%, after PP2 treatment CIPm cells showed a migration rate of 74% at 24 hours. After SRC-I1 treatment, CIPm cells showed migration rates of 62% and 91%, while CIPm cells in control condition completely filled the wound at 24 and 48 hours. So compared to control CIPm cells, PP2 treatment inhibited migration rate with 26% at 24hours, and SRC-I1 treatment with 38% and 9% at 24 and 48 hours, respectively.

Figures 10B and 10D show the migration of CIPm cells in DMSO control condition and after treatment with BEZ and Everolimus. Both inhibitors did not affect migration of CIPm cells compared to migration of CIPm cells in control condition.

The obtained migration rate data are summarized in the table below (table 3).

Table 3. An overview of the obtained migration rate data of CMT-U27 cell line and CIPm cell line in control condition (DMSO) and after treatment with two SRC inhibitors and two mTOR inhibitors. *P*<0.05 is marked as * and indicates a significant difference compared to the DMSO control.

	CMT-U27 24h	CMT-U27 48h	CIPm 24h	CIPm 48h
DMSO	46%	70%	100%	100%
PP2	8% (↓38%) (*)	19% (↓51%) (*)	74% (↓26%)	100%
SRC-I1	17% (↓29%) (*)	35% (↓35%) (*)	62% (↓38%)	91% (↓9%)
DMSO	32%	86%	100%	100%
BEZ	9% (↓23%) (*)	42% (↓44%) (*)	100%	100%
EVE	22% (↓10%) (*)	56% (↓30%) (*)	100%	100%

3.5 Discussion

3.5.1 Cell viability

The cell viability assay was performed in order to examine if the eight compounds related to SRC-I1 affected cell viability of CMT-U27 and CIPm cells. The results showed again that the compounds only decrease cell viability when using relatively high concentrations and that the obtained IC50-values are quite higher than the IC50-values according to manufacturer's information and as described in literature (60)(61)

Hardly any difference was found in sensitivity to the selected eight inhibitors when comparing the cell line CMT-U27 to the cell line CIPm.
We expected a more important role of SRC in CMT-U27 cells than in CIPm cells, because SRC was thought to play a role in the mTOR pathway, as well in the canonical Wnt pathway. Therefore, the expectation was that CMT-U27 cells would be also more sensitive to the SRC-inhibitors Dasatinib and PP2. However, the results did not fit this expectation.

Another unexpected result was that CMT-U27 cells are barely more sensitive to inhibition of EGFR and HER2 (Afatinib), of which HER2 is a factor three upregulated in CMT-U27 cells. As described earlier, binding of a ligand to HER2 leads to activation of the mTOR pathway, thereby promoting cell proliferation. (43-48) Therefore, it seems to be logical that inhibition of this receptor leads to a decreased cell viability in CMT-U27 cells and that CMT-U27 cells would be more sensitive to HER2 inhibition than CIPm cells.

Nevertheless, CMT-U27 cells showed to be 13 times more sensitive to Aurora A inhibition (Aurora A inhibitor 1) and about a factor 11 more sensitive to Aurora B, and to a lesser degree Aurora A, inhibition (Barasertib). Could it be a possibility that Aurora A plays a role in the canonical Wnt pathway?
In gastric cancer cells it has been found that overexpression of Aurora kinase A (AURKA) leads to an upregulated phosphorylation of the protein GSK-3β. As told in the general introduction, GSK-3β is responsible for the phosphorylation of β-catenin, thereby marking it for degradation. However, phosphorylated GSK-3β is kinase inactive and is not able to phosphorylate β-catenin. As a result, β-catenin will not be degraded, leading to an accumulation of β-catenin in the cytosol, followed by a nuclear translocation. (68) The same results were found in colon cancer cells and cervical cancer cells. (69) Furthermore, in ovarian cancer cells it has been found that AURKA also crosstalks with the PI3K/AKT/mTOR pathway. Several studies show that AURKA phosphorylates and inhibits p53, thereby inhibiting PTEN and stimulating the mTOR pathway. (70)

3.5.2 TCF-reporter assay

This TCF-reporter assay showed that the inhibitors Dasatinib, OSI-906 and PP2 significantly inhibit the canonical Wnt activity of CMT-U27 cells.

Unfortunately, we faced a lot of problems with the measurement of the Renilla signal. The Renilla signal serves as a control, since the assumption is that each sample takes in an approximately similar amount of Renilla. This signal is thus supposed to be stable and supposed to induce similar signals in each sample. The TOP and FOP values are divided by the Renilla values, to correct for transfection efficiency. However, our Renilla values were not stable at all and a lot of variation was found in our

Renilla measurements. This made it hard to calculate the Renilla corrected TOP/FOP ratios and to do statistics on it due to the little usable results. Therefore, also the not corrected TOP/FOP ratios were calculated, and statistics were performed on these ratios, because of the larger amount of results. For this assay the Promega's Dual Luciferase Reporter System E1910 kit was used. The half-life time of this kit is quite short, a few minutes. A recommendation could be to use the Promega's Dual Glo E2920 kit. The half-life time of this kit is higher, around two hours. Maybe, this kit can solve the problem with the instability of Renilla.
And unfortunately, the inhibitor Afatinib influenced FOP, while the FOP measurements should be around the same values in each sample. Repetition of the experiment brought the same results every time. Therefore, it was not possible to calculate the TOP/FOP ratios of the cells treated with Afatinib, and unfortunately no conclusions about the effect of Afatinib administration on canonical Wnt activity in CMT-U27 cells could be made.

The inhibitors Dasatinib and PP2, which both have members of the SFK as targets, had the strongest significantly inhibitory effects on the canonical Wnt activity of CMT-U27 cells. So, it seems reliable that SRC is the main player in connecting the mTOR pathway (downstream pathway of the EGF receptors) and the canonical Wnt pathway. As already mentioned, the interaction between EGF receptors and SRC results in the activation of SRC. After activation, SRC becomes tyrosine kinase active, making SRC able to transduce signals to other pathways.
It has been shown that SRC can positively regulate the canonical Wnt pathway via several ways. Yokoyama *et al.* showed that SRC positively regulates the Wnt pathway at the level of Dishevelled 2 (DVL2), which is an important locus for Wnt signaling. SRC docks in the presence of a Wnt signal to the SH3-binding domain of DVL2, leading to the phosphorylation of DVL2. DVL2 then becomes active to suppress GSK-3β activity. As a result, β-catenin is not phosphorylated and will therefore not be degraded. These events make β-catenin able to accumulate in the nucleus, leading to gene transcription. (57)(71) It has also been shown that SRC can phosphorylate specific tyrosine residues in β-catenin, disrupting the interactions with cadherins, so that β-catenin can translocate to the nucleus. (72) Karni *et al*. even showed that activated SRC can directly enhance the synthesis and activity of β-catenin. (73) Other studies also showed that activated SRC can directly interact with β-catenin. (74)(75) Since the role of activated SRC in the Wnt pathway is clear, we assume that the activation of SRC by the EGF receptors also contributes to the positively regulatory role of SRC in the Wnt pathway.
Because of SRC-inhibitors inhibit canonical Wnt activation, it may be useful to treat patients, who receive Everolimus, also with SRC inhibitors to eliminate the stimulatory effect of Everolimus on the canonical Wnt pathway. But, it needs definitely more research to find out if patients benefit from a dual treatment.

The results also show that the inhibitor OSI-906, which targets the type 1 insulin-like growth factor receptor (IGF-1R), significantly inhibits canonical Wnt activity. According to literature, SRC can also interact with IGF-1R, which also disrupts the auto inhibitory interactions and makes SRC active. As mentioned above, activated SRC can contribute to the activation of the canonical Wnt pathway. (58)

Incubation with Aurora A inhibitor 1 and Barasertib did not inhibit canonical Wnt activity of the CMT-U27 cell line. So the results of this TCF-reporter assay do not support the hypothesis derived from the cell viability assay that AURKA could play a role in the Wnt pathway. It is concluded that no direct

relation exists between the viability results of the compounds as measured by MTT and the effects on canonical Wnt signaling as measured by TOP/FOP ratio.

3.5.3 Scratch assay

The scratch assay was performed in order to characterize the effect of SRC- and mTOR inhibitors on the migration of canine mammary tumor cells with high basal Wnt activity (CMT-U27 cell line) and low basal Wnt activity (CIPm cell line).

The scratch assay showed that SRC-I1 and PP2 significantly decrease the migration rate of CMT-U27 cells, but that Everolimus and BEZ235 do not significantly increase the migration rate of CMT-U27 cells.
SRC-I1 and PP2 are both SRC inhibitors and are, as already mentioned earlier, inhibitors of the canonical Wnt pathway. Our hypothesis was that inhibition of the Wnt pathway leads to a decreased migration rate, since inhibition of the canonical Wnt pathway leads to inhibition of EMT. Indeed, we saw a significantly decreased migration rate of CMT-U27 cells, after incubation with SRC inhibitors. One of the target genes of the Wnt pathway, SLUG, induces EMT by down regulating E-cadherin. This down regulation of E-cadherin results in cells that are less connected to each other, making them able to migrate. Therefore, inhibition of the Wnt pathway seems to inhibit EMT via a decreased gene transcription of Slug, which is confirmed by a study of Liu *et al*. (67)(76)

Unexpectedly, the SRC inhibitors also decreased the migration rate of the cells with low Wnt activity (CIPm), although not significant. Since the inhibitors also affect cell proliferation, it could be possible that a decreased cell proliferation has led to a decreased cell migration.
The effect of the inhibitors on cell proliferation could also have contributed to the significant decreased migration rates of the CMT-U27 cells treated with PP2 and SRC-I1. Therefore, it is hard to conclude that the decreased migration rate is only caused by inhibition of the canonical Wnt pathway.

Because mTOR inhibitors also inhibit cell proliferation, it could be that inhibited cell proliferation prevented increased migration rates. Our hypothesis was that CMT-U27 cells would migrate faster after the addition of mTOR-inhibitors, through stimulated canonical Wnt activity. A study of Serra *et al*. showed that mTOR inhibition leads to up regulation of the expression of EGF receptors and their activation. Because SRC can be activated by the EGF receptors, the up regulation and hyper activation of the EGF receptors could be responsible for the further activated Wnt activity in CMT-U27 cells treated with mTOR inhibitors. (77)

The results also showed that CIPm cells migrate faster than CMT-U27 cells. According to the theory of Wnt-driven EMT, CMT-U27 cells should migrate faster than CIPm cells. However, CIPm is a metastatic line, so it is not totally surprisingly that CIPm cells have strong migration capacities. Nevertheless, the driving forces of this migration capacity are not due to elevated Wnt activity.

3.6 Conclusion

The canonical Wnt activity results, as measured by the TOP/FOP assay showed that the compounds Dasatinib, PP2 and OSI-906 significantly decreased the Wnt activity of the CMT-U27 cell line compared to the DMSO control. These results indicate that SRC interacts with the canonical Wnt pathway. Since SRC can be activated by the EGF receptors, it seems obvious that SRC is the

connecting factor between the downstream pathway of the EGF receptors (the mTOR pathway) and the canonical Wnt pathway. The results of the scratch assay also indicate that SRC influences canonical Wnt activity. Addition of the SRC inhibitors PP2 and SRC-I1 resulted in a significant decreased migration rate of CMT-U27 cells, indicating that inhibition of the canonical Wnt pathway leads to inhibition of EMT, which is also confirmed by others (67). Based on the cell viability results it is concluded that no direct relation exists between the viability results of the compounds as measured by the MTT assay and the effects on canonical Wnt signaling.

4. The role of HER2 and HER3 in canonical Wnt activation

4.1 Abstract

Background: Analysis of gene expression levels of canine mammary tumor cell lines showed that high canonical Wnt activity is accompanied by high expression of *HER2* and *HER3* mRNA.

Objectives: The aim of this part of the study was to find out if the upregulation of HER2 and HER3 contributes to the high canonical Wnt activity in the CMT-U27 cell line.

Methods: In the CMT-U27 cell line, HER2 and HER3 were silenced using siRNA. After silencing, the CMT-U27 cells were analyzed for changes in cell viability (MTT assay), canonical Wnt activity (TCF-reporter assay) and gene expression levels on RNA level (qPCR) and protein level (western blot).

Results: Results of the MTT assay and TOP/FOP assay showed that silencing of HER2 and HER3 does not significantly alter cell viability and canonical Wnt activity in the CMT-U27 cell line, when compared to CMT-U27 cells in MOCK control condition. qPCR results showed that HER2 silenced cells contain significant decreased gene expression levels of *Axin2* (at 24h), *BCL2* (at 72h) and *LEF1* (at 72h), and a significant increased expression of *TNFα* (at 72h). HER3 silenced cells showed a significant increased gene expression of *TNFα* (at 24h). At protein level, phosphoSRC was reduced with 46% and 63% in the HER2 and HER3 silenced cells, respectively, when compared to the MOCK control at 72 hours.

Conclusions: Based on the results of cell viability assay, TCF-reporter assay and most qPCR results it is concluded that HER2 and HER3 do not cause the high canonical Wnt activity in the CMT-U27 cell line. However, this study showed also some results which suggest that HER2 and HER3 indeed may influence the canonical Wnt pathway. Nevertheless, the fold changes in gene expression level were quite minimal and the results of the Western blot were based on a single experiment, making it impossible to conclude that HER2 and HER3 play a role in the overactivation of the canonical Wnt pathway. Therefore, repeating the experiments, with siRNAs which possibly induce higher knockdown efficiency, is recommended to obtain more consistent results and more clarity about the possible roles of HER2 and HER3 in the activation of the canonical Wnt pathway. Also experiments with a combination of HER2 and HER3, and silencing of EGFR are recommended.

4.2 Introduction

The EGFR family and their ligands play an important role in mammary development and in breast cancer development. This EGFR family consists of four closely related transmembrane tyrosine kinase receptors: EGFR/HER1, HER2, HER3 and HER4. Binding of EGF-related growth factors to a receptor results in receptor homo- and/or heterodimerization. HER2 and HER3 depend on heterodimerization, since ligands are not able to bind HER2 and since HER3 has no kinase activity. (78) The heterodimer HER2/HER3 is the most potent activator of the PI3K/AKT/mTOR pathway, because HER3 can directly bind to the p85 subunit of PI3K. (44)(79) This pathway is essential for metabolism, proliferation, survival, migration and angiogenesis. (77)

Analysis of gene expression levels of canine mammary tumor cell lines with high and low Wnt activity showed that high canonical Wnt activity is accompanied by high expression of HER2 and HER3. The canine mammary cell lines containing high canonical Wnt activity show a factor three upregulation of HER2 and even a factor 45 upregulation of HER3, when compared to cell lines with low canonical Wnt activity.

So, there is a strong indication that the upregulation of HER2 and HER3 contributes to the high canonical Wnt activity in certain cell lines. As told in the previous chapter, HER2 and HER3 are able to activate SRC, making SRC capable to stimulate the Wnt pathway. Therefore, our hypothesis was that the up regulation of HER2 and HER3 leads to activation of SRC, thereby stimulating the canonical Wnt pathway.

4.2.1 Outline of the study

To test if the upregulated HER2 and HER3 expression is involved in the high activity of the canonical Wnt pathway in the CMT-U27 cell line, HER2 and HER3 were silenced using small interfering RNA (siRNA), also known as silencing RNA and short interfering RNA.

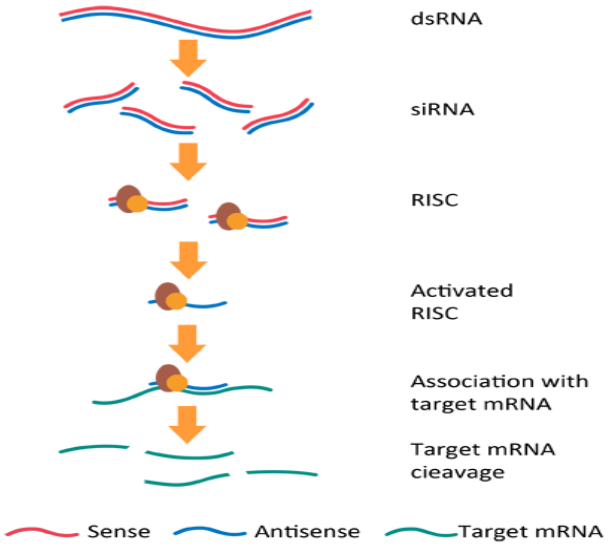

Figure 11. The mechanism behind siRNA. The presence of double stranded (ds) RNA in a cell triggers a mechanism, called RNA interference (RNAi). During RNAi, the enzyme RNA-inducing silencing complex (RISC) binds to the siRNA pairs, and uses one strand of small interfering RNA (siRNA) to bind to mRNA of complementary sequence. As a result, mRNA is degraded, and the expression of the gene encoded by the mRNA is silenced. Adapted from Mocellin S. *et al.* (2004)(80)

When transfecting cells with double stranded (ds) RNA, a mechanism is triggered, which includes a cascade of molecular events known as RNA interference (RNAi). Figure 11 shows the mechanism behind it. The siRNA pairs of a length of ~20 nucleotide pairs bind to the cellular enzyme called RNA-inducing silencing complex (RISC). RISC uses one strand of the siRNA to bind to mRNA of complementary sequence. The nuclear activity of RISC then leads to the degradation of the mRNA, thus silencing the expression of the gene encoded by the mRNA. (80)

After transfection, the HER2 and HER3 silenced cells were analyzed for changes in cell viability (MTT), canonical Wnt activity (TCF-reporter) and gene expression levels on RNA (qPCR) and protein level (Western blot).

4.3 Materials and Methods

4.3.1 siRNA design

The mRNA and genomic sequences for HER2 and HER3 were obtained from the National Center for Biotechnology Information (NCBI) GenBank database (http://www.ncbi.nlm.nih.gov). Then, HER2 (Genbank: AB008451) and HER3 (Genbank: XM_538226) siRNA was designed on the website http://www.dharmacon.com/designcenter/designcenterpage.aspx (DharmaconRNAi technologies, Thermoscientific, Lafayette, USA). There was no cross-silencing of non-target genes found by blasting the siRNA designed sequences against the canine genome database. The sequence of the HER2 siRNA duplex is as follows: sense 5'CUUCGAAGCCUCACAGAGAUU 3' and antisense 5' UCUCU GUGAGGCUUCGAAGUU 3'. The sequence of the HER3 siRNA duplex is sense 5' GGACAAGAGUGGACGGCAGUU 3' and antisense 5'CUGCCGUCCACUCUUGUCCUU 3'.
MOCK siRNA (ON-Target plus non-targeting pool species H (human), M (mouse) and R (Rat)) was used as negative control for the siRNA experiments. Changes in mRNA or protein levels in the MOCK treated cells reflect a baseline cellular response that can be compared to the levels in cells treated with target-specific siRNA. So this control distinguishes sequence-specific silencing from non-specific effects. Untreated (control) cells were used to determine baseline cell viability and target gene level.

4.3.2 Cell culture and transfections

Only the cell line CMT-U27 was used in this study. All cell culture handlings were performed as described in chapter 3.

First, an optimalisation experiment with siGLO green transfection indicator (#D-001630-01-05, Dharmacon) was performed to determine the optimal concentrations of the siRNA, MOCK and the Dharmafect Duo transfection reagent (#T-2010-03, Dharmacon) required for silencing transfection. CMT-U27 cells were seeded in 24-wells Primaria plates (#353847, Corning) at a density of 125.000 cells/ml DMEM/F12 with 10% FCS.
After obtaining the optimal concentrations of siRNA and MOCK (50 nM) and Dharmafect Duo (2 µl), the silencing experiments with HER2 and HER3 siRNA were performed.

On the first day, the CMT-U27 cells were seeded in several plates; 24-wells Primaria plates for TOP/FOP measurement and RNA isolation, 6-wells Primaria plates for protein isolation and 96-wells plates for MTT assay. The seeding densities were 125.000 CMT-U27 cells/ml for the 24-wells plates, 600.000 cells/3 ml for the 6-wells plates and 15.000 cells/100 µl for the 96-wells plates.

After 24 hours, CMT-U27 cells were transfected with 2 µl transfection reagent Dharmafect Duo, 50 nM siRNA or MOCK, 800 ng TOP or 800 ng FOP and 0.5 ng β- Actin Renilla. Before transfection, medium was removed and 400 µl DMEM/F12 + 10% FCS was added to the 24-wells plates and 1.6 ml to the 6-wells plates. Medium of the 96-wells plates was not removed.
After that, the transfection (containing either MOCK, HER2 or HER3 siRNA, and TOP or FOP) and Dharmafect Duo mixes were made. After 5 minutes incubation on room temperature an equal amount of the Dharmafect Duo mix was added to the transfection solutions. The solutions were mixed gently and then incubated for 20 minutes at room temperature.
After icubation, 100 µl was added to the 24-wells plates, 400 µl to the 6-wells plates and 25 µl to the 96-wells plate.

4.3.3 Cell viability and TCF-reporter assay

48 hours after transfection, MTT assay and TCF-reporter assay were performed, according to the protocols described in the previous chapter (3.3.2 and 3.3.3). The experiments were performed three times, with an average of 4 wells per condition for the TOP/FOP assay (n=12) and an average of 6 wells per condition for the MTT assay (n=18).

4.3.4 RNA isolation and cDNA synthesis

24, 48 and 72 hours after transfection, RNA was isolated using the RNeasy Mini Kit (#74104, Qiagen, Venlo, The Netherlands) according to manufacturer's instructions. An average of 18 wells per condition was used for the 24 hours isolation, and an average of 12 wells per condition for the isolation after 48 and 72 hours. Two wells were pooled together, so the final numbers per condition were nine for the 24 hours samples, and six for the 48 and 72 hours samples. DNAse treatment was performed on all samples to prevent contamination with DNA. The absorbance was measured with a Nanodrop (Thermo Scientific NanoDrop ND-1000, Isogen Life Sciences, De Meern, The Netherlands) spectrophotometer, thereby using the ratio 260/280 to assess the purity of the RNA. A ratio of ~2.0 was indicated as ''pure'' RNA. The isolated RNA was stored at -20°C until further amplification.
cDNA was made from 500 ng RNA using the iScript cDNA synthesis kit (#1708890, Bio-Rad, Hercules, CA, USA), according to manufacturer's protocols. Also the cDNA was stored at -20°C until qPCR experiments were performed.

4.3.5 Gene expression

qPCR was performed on the total of 84 samples, to determine any changes in gene expression levels. To correct for differences in cDNA concentration, the expression levels of the target genes were normalized to the expression levels of endogenous reference genes. 25 target genes and 14 reference genes were measured, as shown in table 4. Appendices 9B and 9C show the primer pairs which were used. The list of abbreviations can be found in Appendix 9A.
The target genes were selected on the criterion that they are connected to the Wnt pathway and/or the mTOR pathway.

Table 4. List of reference and target genes used for qPCR.

Reference genes	Target genes
B2M	Axin2
GAPDH	β-Catenin
GUSB	BCL2
HMBS	cMET
HNRPH	cMYC
HPRT	Cyclin D1
RPL8	E-cadherin
RPL13	EGFR
RPS5	HER2
RPS19	HER3
SDHA	HER4
SRPR	HSP90a
TBP	ID1
YWHAZ	ID2
	LEF1
	MUC1
	NCOA3
	NRG1
	PGR
	RAC1
	RAC1B
	SLUG
	SRC
	TGFα
	TNFα

A pool of all control samples was made to create a four-fold dilution series for the use as a standard. The remaining cDNA was 50 times diluted with milliQ.
qPCR was performed on a 384 Real-Time System (Bio-Rad), using 384-well hard sheet PCR plates and SYBR GREEN as Fluorophore (Bio-Rad). According to manufacturer's protocol, each qPCR reaction was performed in a total reaction volume of 10 µL. All reactions were performed in duplicate and negative controls (only containing milliQ) served to assess the specificity and to exclude any contamination.
Data analysis was accomplished with CFX Manager 3.0 software (Bio-Rad). The amplification efficiency of each standard dilution series was calculated and values between 95% and 105% were accepted for reference genes and values between 90% and 110% were approved for target genes. It was also checked if the melt curve

gives one peak at the correct melting temperature, and if the negative controls did not give a Ct-value and a melt curve. Reference genes were tested in geNorm. The 2-ΔΔCT method was used to calculate relative expression levels for each of the target genes. (81).

4.3.6 Protein isolation

Protein was isolated after 24, 48 and 72 hours. To 1 ml RIPA 30 µl Aprotinin (#A6279, Sigma-Aldrich), 10 µl PMSF (#93482, Sigma-Aldrich) and 10 µl Sodium Orthovanadate (#S6508, Sigma-Aldrich) were added, to create the solution RIPA+.

Medium of the cells was removed and cells were washed with 3 ml cold HANKS. Then the cells were placed on ice and 250 µl cold RIPA+ was added to the cells. After that, the cells were scraped and pipetted into Eppendorf tubes. These tubes were then rotated at 4 °C for 30 minutes and after that spinned down in a cooled centrifuge (4 °C) at 15000 rpm for 30 minutes. Thereafter, the protein concentrations were determined using the Bio-Rad Dc Protein Assay (Bio-Rad, Veenendaal, The Netherlands).

4.3.7 Western blot

20 µg protein from total cell lysates was subjected to SDS-page and applied to 7.5% Criterion TGX gels (#5671023, Bio-Rad) and 10 µl of a prestained recombinant precision plus protein dual color standard (#1610374, Bio-Rad) was loaded. The gels ran at 80 volt for 30 minutes to concentrate and carefully load the samples in the running gel. Thereafter, the gels ran at 100-150 volts for as long as needed for sufficient separation of the marker bands. After electrophoresis, the gel was transferred to a cassette and was blotted for one hour at 100 volt.

After blotting, the membrane was blocked for one hour in TBST 0.1% + 4% Amersham ECL Blocking agent solution (#RPN2125, GE Healthcare Life Sciences, Eindhoven, The Netherlands) by swinging on a rotating band at room temperature.

After blocking, the membranes were overnight incubated with primary antibodies by swinging on a rotating band at 4°C. The primary antibodies were dissolved in TBST 0.1% + 4% BSA (#A3059, Sigma-Aldrich) (table 5). β-Actin was used as a loading control.

Table 5. Primary antibodies used for Western blot.

Antibody against	Type	Dilution	#number and firma
β-Actin	Mouse monoclonal	1:2000	MS-1295-P1 (Thermo Scientific, Landsmeer, The Netherlands)
HER2	Rabbit polyclonal	1:500	PA5-14635 (Pierce, Thermo scientific)
HER3	Goat polyclonal	1:2500	PA1-86644 (Thermo Scientific)
PhosphoSRC	Rabbit polyclonal	1:750	Ab79308 (Abcam, Cambridge, UK)
SRC	Rabbit polyclonal	1:1000	Ab105215 (Abcam)

After overnight incubation with primary antibodies, the membranes were washed 3x 10 minutes in TBST 0.1%. Thereafter, the membranes were incubated for one hour in the HRP conjugated secondary antibodies, dissolved in TBST 0.1% + 2x BSA 1% (table 6).

Table 6. Secondary HRP-conjugated antibodies used for Western blot.

Antibody against	Type	Dilution	#number and firma
β-Actin	Anti-mouse	1:20.000	HAF007 (R&D Systems, Minneapolis, USA)
HER2	Anti-rabbit	1:20.000	HAF008 (R&D Systems)
HER3	Anti-goat	1:20.000	HAF109 (R&D Systems)
pSRC	Anti-rabbit	1:20.000	HAF008 (R&D Systems)
SRC	Anti-rabbit	1:20.000	HAF008 (R&D Systems)

After one hour incubation, the membranes were washed 3x 5 minutes in TBST 0.1%. Amersham ECL Select Western Blotting Detection Reagent (#RPL2235, GE Healthcare) was added to the membrane and the bands were visualized using the GelDoc2000 (Bio-Rad).
With the ImageJ Analysis software, version 1.4.7, densities were measured, corrected for the background and related to β-Actin as a loading control.

4.3.8 Statistical analysis

Statistical analysis was conducted using IBM SPSS Statistics version 22 software (SPSS Benelux). Data were normally distributed, so the one-way ANOVA and the post-hoc Bonferroni tests were applied. A *P*-value <0.05 was considered as significant when compared to the MOCK control, which is indicated with an asterisk (*) in the figures. Results were compared to the MOCK control instead of the control, because we wanted to distinguish sequence-specific changes (caused by siRNA) from non-specific changes.

4.4 Results

4.4.1 Knockdown of HER2 and HER3 on gene expression level

At 24 hours, HER2 was knocked down to 36% when compared to the control and to 41% when compared to the MOCK. At 48 hours, a knockdown to 44% and 31%, when compared to the control and MOCK respectively, was found. At 72 hours, HER2 was knocked down to 48% and 36% when compared to the control and MOCK (Fig. 12A).

At 24 hours, a knock down to 32% and 59% was found when comparing HER3 to the control and MOCK. At 48 hours, HER3 was knocked down to 42% and 46% compared to the control and MOCK, respectively. At 72 hours, HER3 showed a knock down to 46% and 51%, when compared to CMT-U27 cells in control and MOCK conditions (Fig. 12B).

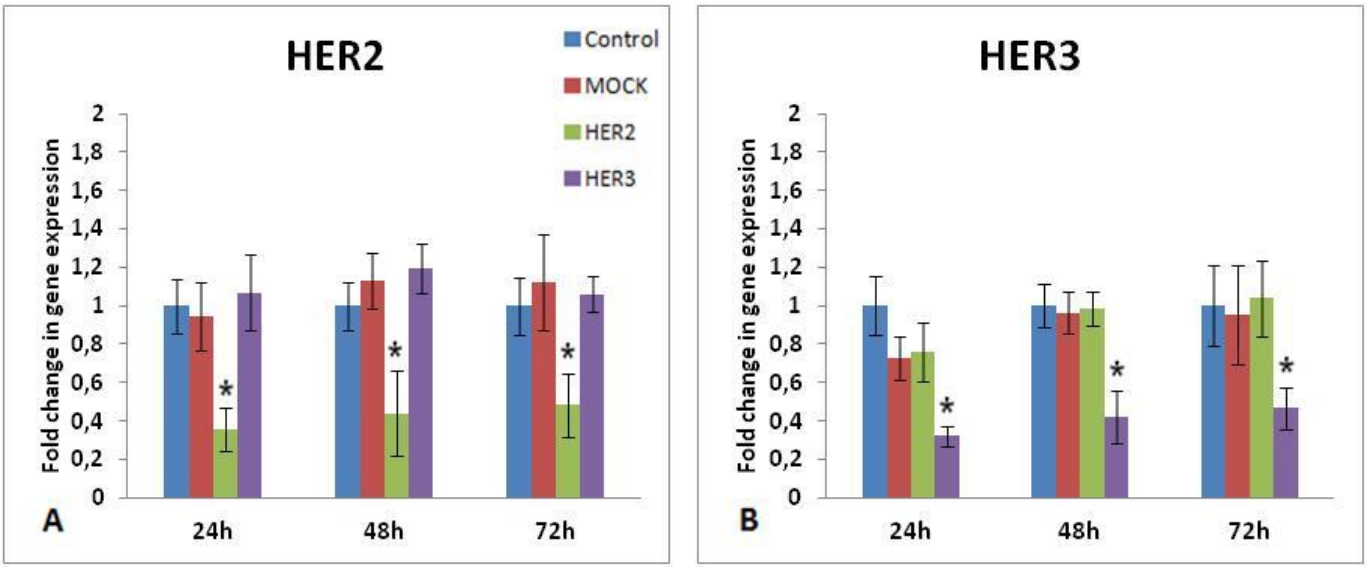

Figure 12. Gene expression of HER2 and HER3 in CMT-U27 cell line in control conditions (control and MOCK) and after silencing of HER2 and HER3. The cell line was grown for 24, 48 and 72 hours in the presence of MOCK, HER2 and HER3 siRNA. After incubation RNA was isolated and the relative expression of HER2 (**A**) and HER3 (**B**) was measured by quantitative RT-PCR. Results expressed as % of control (set to 100%) are the mean (±SEM) of nine samples out three independent experiments (24 hours) and the mean of six samples out two independent experiments (48 and 72 hours). *P*<0.05 is marked as * and indicates a significant difference compared to the MOCK control.

4.4.2 Knockdown of HER2 and HER3 on protein level

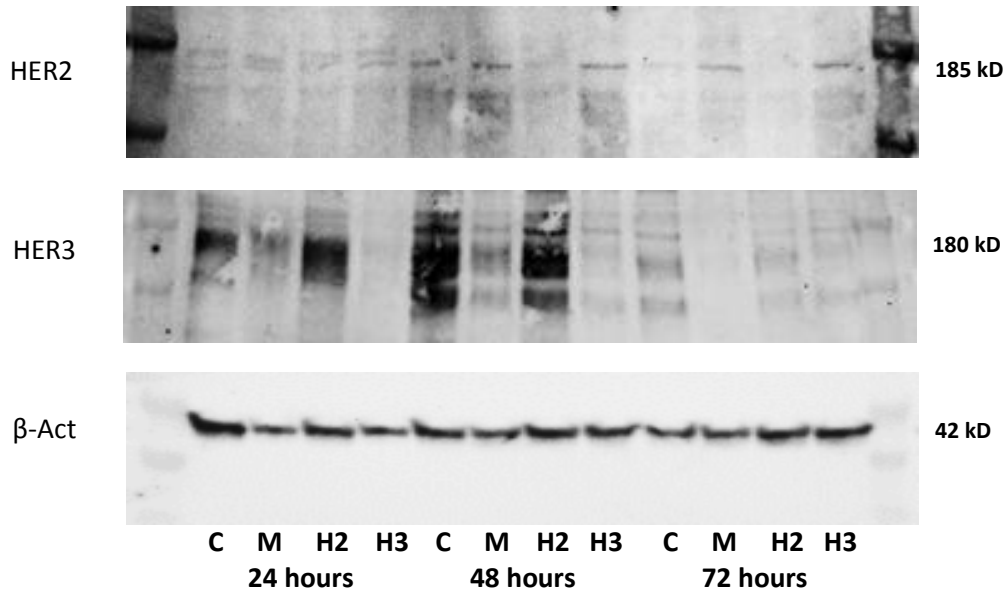

Figure 13. Protein levels of HER2, HER3 and β-Actin in CMT-U27 cell line in control conditions (control and MOCK) and after silencing of HER2 and HER3. The cell line was grown for 24, 48 and 72 hours in the presence of MOCK, HER2 and HER3 siRNA. Total protein was isolated with RIPA buffer and 20 µg protein was used for Western blot analyses. Blots were probed with total antibodies for HER2, HER3 and β-Actin. C: Control; M: MOCK; H2: HER2; H3: HER3

After correction for the background and β-Actin as a loading control, the Western blot showed an increase of HER2 on protein level of 7% at 24 hours, a knockdown to 43% at 48 hours and a knockdown to 64% at 72 hours, when compared to the control (set to 100%). When compared to the MOCK, an increase of HER2 protein level of 31% at 24 hours, a knockdown to 41% at 48 hours and a knockdown to 28% at 72 hours was found (Fig. 13).

The Western blot showed a HER3 knock down to 13% at 24 hours, a knock down to 7% at 48 hours and a knock down to 33% at 72 hours, when compared to the control (set to 100%). When compared to the MOCK, a HER3 protein knock down to 16% at 24 hours, a knock down to 19% at 48 hours and an increase of 109% at 72 hours was demonstrated (Fig. 13).

4.4.3 Cell viability

Comparing the results of the siRNA treated cells to the cells in MOCK control condition, the cell viability of the HER2 silenced cells and the HER3 silenced cells was not significantly changed (Fig. 14).

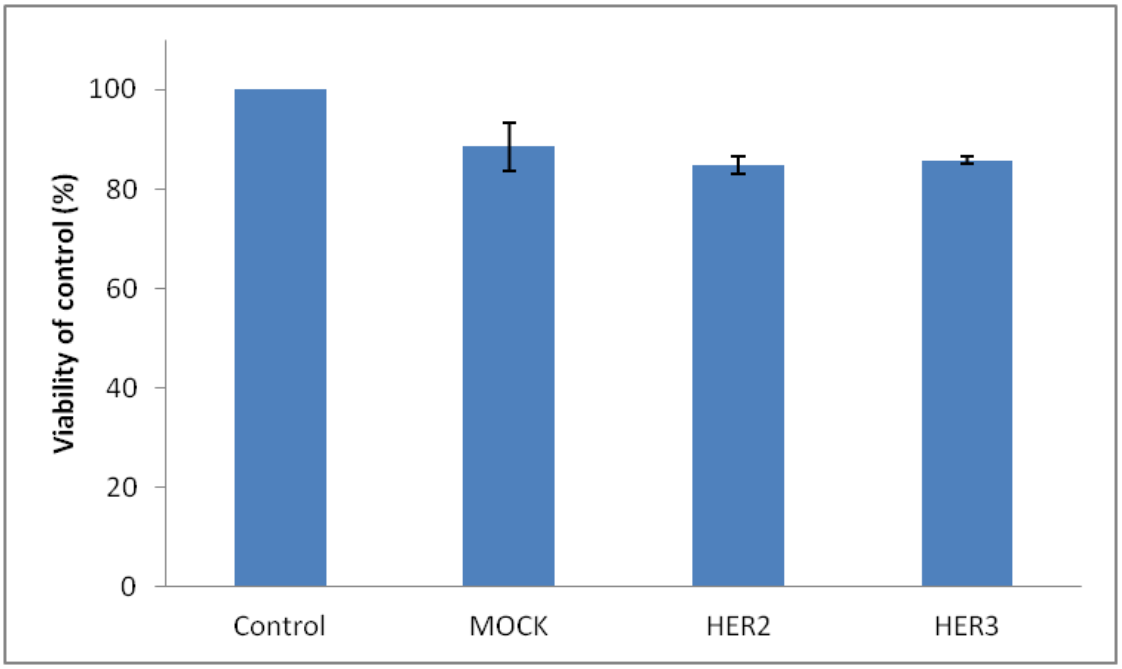

Figure 14. Cell viability of CMT-U27 cell line in control conditions (control and MOCK) and after silencing of HER2 and HER3. CMT-U27 cells were grown for 48 hours in the presence of MOCK, HER2 or HER3 siRNA. After 48 hours cell viability was measured with a MTT assay. Results expressed as % of control (set to 100%) are the mean (±SEM) of 18 samples out three independent experiments (n=18). No significant differences were found compared to the MOCK control.

4.4.4 TCF-reporter assay

The HER2 silenced cells did not show a significantly decreased canonical Wnt activity, when compared to CMT-U27 cells in MOCK control condition. The HER3 silenced cells showed a significantly increased Wnt activity when compared to the MOCK, with an increase of 62% (Fig. 15).

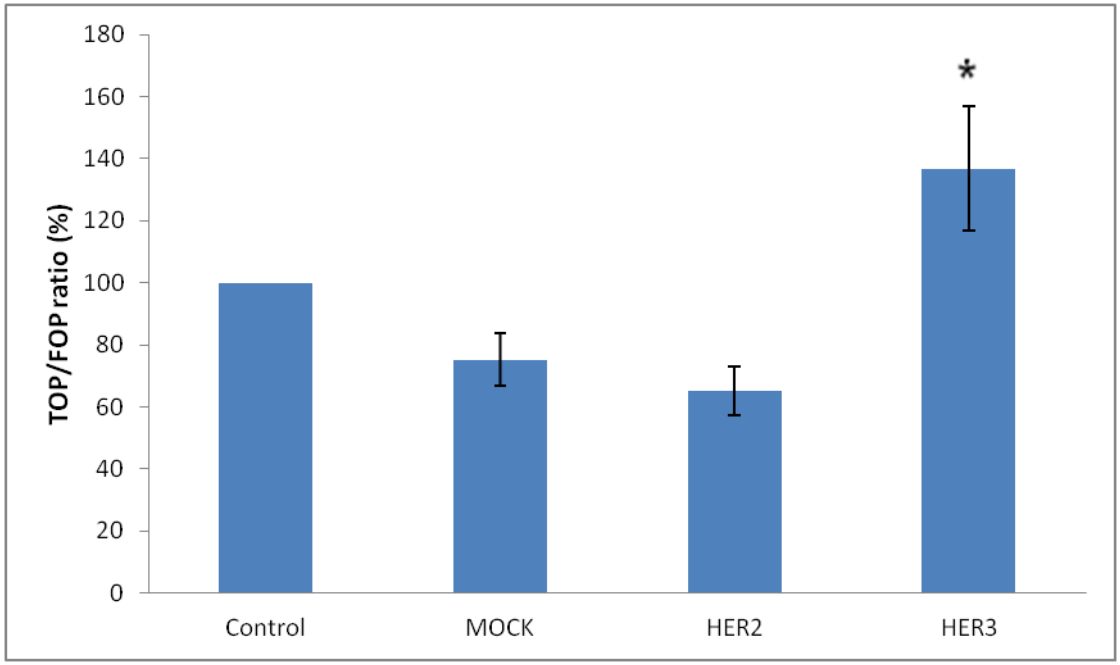

Figure 15. Canonical Wnt activity of CMT-U27 cell line in control conditions (Control and MOCK) and after silencing of HER2 and HER3. The cell line was grown for 48 hours in the presence of MOCK, HER2 or HER3 siRNA. After 48 hours TOP/FOP ratio was measured with a Dual-Luciferase assay. Results expressed as % of control (set to 100%) are the mean (±SEM) of nine samples out three independent experiments (n=9). Results are corrected for transfection efficiency. *P*<0.05 is marked as * and indicates a significant difference compared to the MOCK control.

4.4.5 Gene expression

14 reference genes were measured, but after geNorm data analysis it was concluded to calculate with the following 11 reference genes: RPS5, RPS19, RPL8, RPL13, SDHA, HNRPH, YWHAZ, TBP, SRPR, GUSB and HMBS, with a Pairwise Variation of <0.04. In Appendix 8D the geNorm data analysis results can be found.

Of the 25 target genes measured, only the target genes Axin2, BCL2, LEF1 and TNFα were significantly altered by silencing of HER2 and HER3, when compared to the MOCK (Fig. 16).
At 24 hours, HER2 silenced cells showed a significantly lower expression of Axin2, when compared to the MOCK cells (1.3-fold downregulation). Significant changes in Axin2 expression level were no longer found at 48 and 72 hours (Fig. 16A).
As shown in figure 16B, no significant differences were found in the gene expression level of BCL2 at 24 and 48 hours, when comparing the HER2 and HER3 silenced cells to the MOCK control cells. However, at 72 hours, the CMT-U27 cells treated with HER2 siRNA showed a significantly lower gene expression of BCL2, when compared to the MOCK control (1.5-fold downregulation).
At 24 and 48 hours, the gene expression level of LEF1 was not significantly altered by silencing of HER2 or HER3. Nevertheless, at 72 hours, the HER2 silenced cells showed a significantly lower LEF1 expression when compared to the MOCK cells (1.3-fold downregulation) (Fig. 16C).

At 24 hours, the HER3 silenced cells showed a significantly higher gene expression of TNFα, when compared to the MOCK cells (1.8-fold increase), as shown in figure 16D. At 48 hours, no significant differences were found for both the HER2 and HER3 silenced cells. At 72 hours, the HER2 silenced cells showed a significant increase of TNFα, when compared to the MOCK cells (3.6-fold increase).

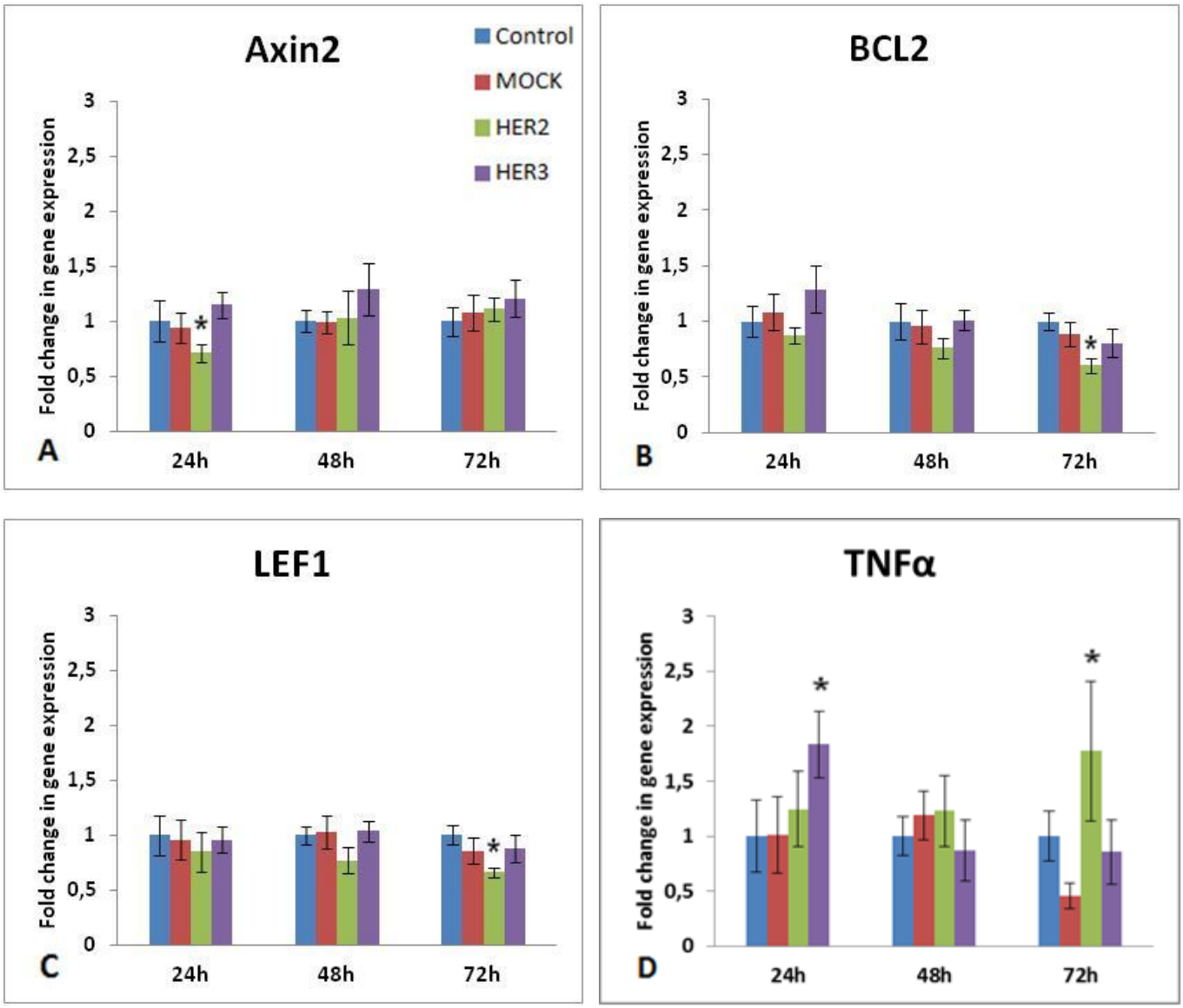

Figure 16. Gene expression of target genes in CMT-U27 cell line in control conditions (Control and MOCK) and after silencing of HER2 and HER3. The cell line was grown for 24, 48 and 72 hours in the presence of MOCK, HER2 or HER3 siRNA. After incubation RNA was isolated and the relative expression of several target genes, Axin2 (**A**), BCL2 (**B**), LEF1 (**C**) and TNFα (**D**) was measured by quantitative RT-PCR. Results expressed as % of control (set to 100%) are the mean (±SEM) of nine samples out three independent experiments (24 hours) and the mean of six samples out two independent experiments (48 and 72 hours). *P*<0.05 is marked as * and indicates a significant difference compared to the MOCK control.

Expression levels of the target genes β-catenin, cMET, cMYC, CyclinD1, E-cadherin, EGFR, HER4, HSP90α, ID1, ID2, MUC1, NCOA3, NRG1, PGR, RAC1, RAC1B, SLUG, SRC and TGFα were not significantly changed by silencing of HER2 or HER3, when compared to cells in MOCK condition. The graphs of the not significantly altered target genes can be found in Appendix 8E (Fig. 20)

4.4.6 Protein expression

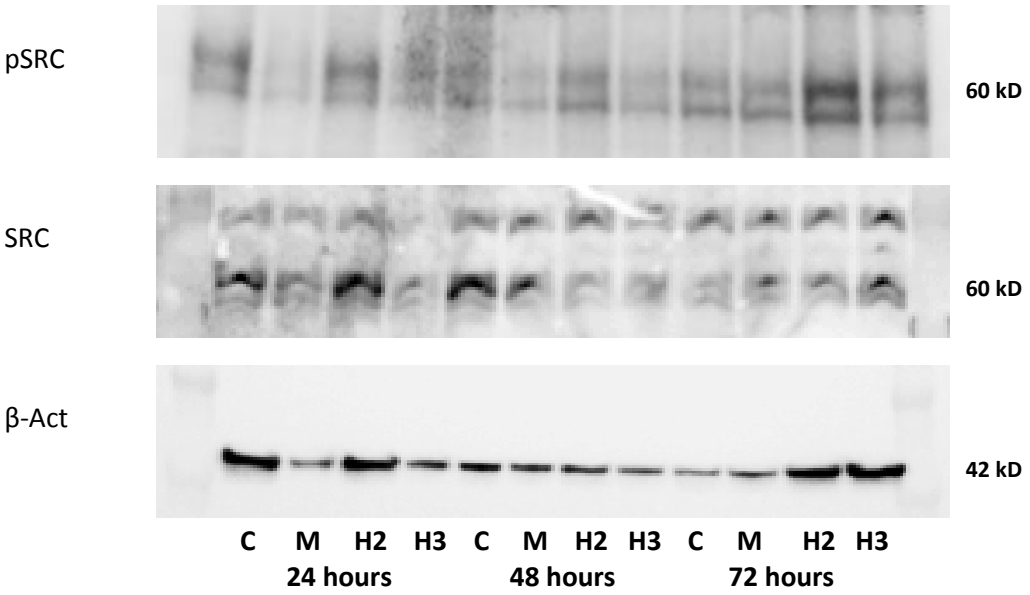

Figure 17. Protein levels of pSRC, SRC and β-Actin in CMT-U27 cell line in control conditions (control and MOCK) and after silencing of HER2 and HER3. The cell line was grown for 24, 48 and 72 hours in the presence of MOCK, HER2 or HER3 siRNA. Total protein was isolated with RIPA buffer and 20 µg protein was used for Western blot analyses. Blots were probed with total antibodies for HER2, HER3 and β-Actin. pSRC: phosphorylated SRC; C: Control; M: MOCK; H2: HER2; H3: HER3

After correction for the background and β-Actin as a loading control, the Western blot showed the following changes in protein levels of pSRC when comparing the HER2 silenced cells to the MOCK: a reduction of 20% at 24 hours, an increase of 40% at 48 hours and a reduction of 46% at 72 hours.
The HER3 silenced cells showed an increase in pSRC protein expression of 20% at 24 hours, an increase of 29% at 48 hours and a reduction of 63% at 72 hours (Fig. 17).

After correction for the background and β-Actin as a loading control, the Western blot of SRC showed that knock down of HER2 results in a reduction in SRC protein expression of 11% at 24 hours, a reduction of 70% at 48 hours and a reduction of 58% at 72 hours.
Knock down of HER3 altered SRC protein expression with a reduction of 48% at 24 hours, a reduction of 40% at 48 hours and a reduction of 49% at 72 hours (Fig. 17).

4.5 Discussion

4.5.1 Cell viability

Compared CMT-U27 cells in control condition, both the HER2 and HER3 silenced cells showed significantly decreased cell viability. However, compared to the MOCK control cells, cell viability of both HER2 and HER3 silenced cells was not significantly decreased. Therefore, we cannot conclude that the decreased cell viability in HER2 and HER3 silenced cells is specifically due to the knockdown. HER2 and HER3 are both receptors upstream of the mTOR pathway. The mTOR pathway plays an important role in cell survival. The Wnt pathway also regulates cell proliferation. (82)(83) Therefore, we expected that silencing of HER2 and HER3 would lead to decreased cell viability. However, this MTT assay does not fit this expectation. Because the mTOR pathway could be activated by signals of several receptors, it could be possible that silencing of only one of the receptors does not result in a strong effect on cell viability.

4.5.2 TCF-reporter assay

This TOP/FOP assay showed that HER2 knockdown does not significantly decrease canonical Wnt activity of CMT-U27 cells, when compared to cells in MOCK control condition. The HER3 silenced cells showed a significantly increased canonical Wnt activity when compared to the control cells, as well when compared to the MOCK treated cells.

As explained earlier, HER2 and HER3 can activate SRC, making SRC able to stimulate the canonical Wnt pathway. Therefore, we expected a decreased TOP/FOP ratio of the HER2 and HER3 silenced CMT-U27 cells. Unfortunately, the results of this assay do not fit this expectation. HER2 knockdown had some inhibitory effect on canonical Wnt activity, but also MOCK administration resulted in a decreased Wnt activity. Therefore, it is not possible to conclude that the inhibition of canonical Wnt activity is specifically caused by HER2 knockdown.

HER3 knockdown showed a significantly stimulatory effect on basal Wnt activity of CMT-U27 cells. This increase seems to be caused by decreased FOP values rather than increased TOP values. FOP values are supposed to be stable and should not be influenced by any treatments. Therefore, increased TOP/FOP ratios should be the result of increased TOP values, instead of decreased FOP values. Therefore, it is also impossible to conclude that HER3 silencing stimulates the canonical Wnt pathway.

In conclusion, this TCF-reporter assay showed that HER2 and HER3 silencing does not result in (significantly) decreased canonical Wnt activity in the CMT-U27 cell line. So we assume that the upregulated HER2 and HER3 expression is not the cause of the upregulation of the canonical Wnt pathway in CMT-U27 cells.

4.5.3 Gene expression

Comparing the qPCR results of HER2 silenced cells to CMT-U27 cells in MOCK control condition, significant decreases of the target genes Axin2 (at 24 hours), BCL2 (at 72 hours), LEF1 (72 hours), and a significant increase of the gene expression of TNFα (72 hours) were found. Although significant, most fold changes were quite minimal, around 1.3-fold to 1.8-fold down/upregulation. However, the HER2 silenced cells showed a 3.6-fold upregulation of TNFα.

Axin2 is an important component and negative regulator of the canonical Wnt pathway. It is part of the destruction complex, which promotes phosphorylation and degradation of β-catenin in the absence of a Wnt signal. The HER2 silenced cells showed a significantly decreased gene expression

level of Axin2 at 24 hours. According to the fact that Axin2 is a negative regulator of the Wnt pathway, downregulation of Axin2 results in reducing this negative regulation, thereby inhibiting the degradation of β-catenin. As a result, the Wnt activity increases. However, the TOP/FOP assay did not show an increased Wnt activity of the HER2 silenced cells. Also no literature is available about a possible interaction between HER2 and Axin2. (84)

BCL2 is an anti-apoptotic protein, and according to literature there is evidence for a connection between the PI3K/mTOR pathway and the BCL2 family. For example, it has been shown that the PI3K/mTOR pathway targets members of the BCL2-family by phosphorylation and stimulates the expression of the anti-apoptotic protein BCL2. (85) The PI3K/mTOR pathway is a downstream pathway of HER2 and HER3. Therefore, silencing of HER2 and HER3 could result in inhibition of the PI3K/mTOR pathway, thereby inhibiting BCL2 expression. Literature also shows that the Wnt pathway can regulate BCL2. (86)

LEF1 showed a significant decrease at 72 hours in HER2 silenced cells. LEF1 is a member of the TCF/LEF family of transcription factors. After stabilization, β-catenin translocates to the nucleus and binds to members of the TCF/LEF family, thereby stimulating transcription of target genes. Literature shows that (high) LEF1 expression contributes to the high canonical Wnt activity in the CMT-U27 cell line. (52) Filali *et al*. showed that activation of the LEF1 promoter is β-catenin-dependent. (87) HER2 can possibly activate β-catenin via SRC. So these findings indicate that HER2 may influence LEF1 expression indirectly via SRC.

At 72 hours, HER2 silenced cells showed a significantly increased expression of TNFα. TNFα is one of the two well-known tumor necrosis factors and is involved in inflammation reactions. Dysregulation of TNFα production has been implicated in several diseases, including cancer. However, not much is known about a possible role of TNFα in breast cancer. Recently, it has been shown that the Wnt pathway can be involved in inflammation and that β-catenin plays a role in it. For example, β-catenin is able to reduce TNFα release. (88) When we assume that HER2 can activate SRC and that activated SRC can activate β-catenin, it is possible that HER2 silencing results in a reduction of activated β-catenin, thereby promoting TNFα release. But it needs definitely more research to find out if TNFα plays a role in breast cancer.

qPCR results of the HER3 silenced cells showed a significant increase of TNFα (24 hours) when compared to cells in MOCK control condition.

Because HER3 can also activate SRC, it is possible that HER3 silencing can also result in increased TNFα release, via the same way as described above. (88)

4.5.4 Protein expression

Western blot results of phosphoSRC showed that pSRC protein level reduced at 72 hours in both HER2 silenced cells (with 46% when compared to the MOCK) and HER3 silenced cells (with 63%).

Our hypothesis was that HER2 and HER3 are capable to phosphorylate SRC, and thereby activating it. According to this hypothesis, HER2 and HER3 knockdown should lead to reduced pSRC protein levels. Indeed, the results showed a reduction of phosphorylated SRC at 72 hours.

However, results of HER2 and HER3 silenced samples did not show a reduction of pSRC protein expression at 24 and 48 hours. This could be explained by the fact that it takes some time before

knockdown affects protein level. However, since we faced problems with succeeding Western blot, the results are obtained from an only once performed experiment, making it necessary to repeat the western blot to draw any conclusions.

Western blot of SRC showed that knock down of both HER2 and HER3 results in reduced SRC protein expression. We did not expect changes in SRC protein expression in the HER2 and HER3 silenced cells. It has been shown that HER2 and HER3 can phosphorylate SRC, thereby turning SRC into an active state. Indeed, we saw altered expression levels of pSRC. But non-phosphorylated SRC should not be influenced by HER2 and HER3 knockdown, since HER2 and HER3 do not influence transcription of SRC. Because Western blot was performed only once, more research and a repetition of the experiment are recommended to draw any conclusions.

4.6 Conclusion

The results of measurement of cell viability and Wnt activity did not show significantly important differences when compared to CMT-U27 cells in MOCK control condition. qPCR results showed that, of the 25 target genes tested, only 4 target genes showed significantly altered gene expression levels, namely *Axin2*, *BCL2*, *LEF1* and *TNFα*. But although significant, the fold changes were quite minimal. Western blot showed reduced pSRC protein expression at 72 hours. However, this was an only once obtained result, since we faced problems with succeeding of Western blot. So, all experiments did not show big differences between the silenced cells and the MOCK control cells.

Thus, although there was an association found between high basal Wnt activity and overexpression of *HER2* and *HER3* mRNA, silencing of these messages did not result in downregulation of the basal Wnt activity. In previous research it was found that treatment with SRC inhibitors resulted in significant reduction of Wnt activity, whereas mTOR inhibitors resulted in increased Wnt activity. Possible explanations are: 1) Insufficient downregulation of increased HER2 and HER3 expression to result in decreased Wnt activity, 2) A combination of decreased SRC and mTOR activity resulting in an overall null effect, and 3) HER2/HER3 independent activation of SRC by mutations of downstream effectors of the HER2/HER3 pathway.

Therefore, some recommendations are thought to obtain possibly better results. Maybe, the level of knockdown was not high enough to cause strong effects. We saw a reduction in gene expression level of HER2 of approximately 60% when compared to the control cells and about 50-60% when compared to the MOCK, respectively. The HER3 silenced cells also showed a reduction of about the 50-60% on RNA level. On protein level, the HER2 silenced cells showed, when compared to the MOCK, a knockdown to 41% and 28% at 48 and 72 hours, respectively. The HER3 silenced cells showed a HER3 knockdown to 16% and 19% at 24 and 48 hours, respectively. So, the HER3 siRNA induced stronger effects on protein level than the HER2 siRNA. The HER2 siRNA had moderate effects on protein level, so designing a new HER2 siRNA can probably lead to better results.

Another possible improvement could be to lengthen the time period between transfection and obtaining results. A possible explanation why no significant decreases in cell viability and canonical Wnt activity were observed could be that both assays were measured too early. Both assays were measured 48 hours after transfection. It takes some time after transfection before effects can be noticed, because protein levels are not immediately affected by transfection. Because gene transcription is dependent on proteins levels, it takes also some time before target genes are

influenced by silencing effects. Therefore, it could be a recommendation to perform the MTT and TOP/FOP assays 72 hours after transfection instead of 48 hours after transfection.

Using another MOCK could also possibly lead to better results. The MOCK we used, affected cell viability, canonical Wnt activity, gene expression levels and protein levels. Often, the results showed a significant difference when compared to CMT-U27 cells in control condition, which only received transfection reagent, but not when compared to the MOCK treated cells. Therefore, it was hard to conclude that effects are sequence-specific effects due to the silencing of HER2 or HER3. According to manufacturer's information, the MOCK we used consists of sequences which contain at least four mismatches to any human, mouse and rat genes. A recommendation could be to use a MOCK control which is also tested for matches against the canine genome, such as the Qiagen's AllStars Negative Control siRNA, which has no homology to any known mammalian gene.

5. General discussion

The first part of this Honours Programme research, which was described in chapter 3, focused on the interaction between the downstream pathway of the EGF receptors (the mTOR pathway) and the canonical Wnt pathway. To test which kinase could be responsible for connecting both pathways to each other, several inhibitors with different targets were added to the cells. The most important finding was that the SRC inhibitors Dasatinib and PP2 significantly inhibited canonical Wnt activity of CMT-U27 cells. Also the inhibiter OSI-906, with the IGF-1R as target, significantly inhibited canonical Wnt activity of the CMT-U27 cells. Since the inhibition of IGF-1R can possibly lead to a reduced activation of SRC, these results point to SRC as the prominent connecting factor between the two pathways. Also the results of the migration assay point to an important role of SRC in the canonical Wnt pathway. The migration assay also showed that inhibition of the canonical Wnt pathway results in a decreased migration rate of CMT-U27 cells, indicating that the Wnt pathway plays indeed an important role in migration. However, no direct relation exists between the viability results of the compounds as measured by MTT and the effects on canonical Wnt signaling.

In the second part of this research year we performed knockdown of HER2 and HER3, using siRNA, with the goal to better understand the relationship of the upregulation of HER2 and HER3, and the activation of the canonical Wnt pathway in the cell line CMT-U27. According to the facts that the interaction of HER2 and HER3 with SRC leads to the activation of SRC, and that activated SRC contributes to the activation of the canonical Wnt pathway, it seemed plausible that HER2 and HER3 indirectly activate the canonical Wnt pathway, via SRC.

However, based on the results of this part of the research, we conclude that HER2 and HER3 do not cause the high canonical Wnt activity in the CMT-U27 cell line. Cell viability assays and TCF-reporter assays showed no significant decreases in cell viability and Wnt activity in HER2 and HER3 silenced cells when compared to the MOCK treated cells. Also HER2 and HER3 knockdown showed no strong effects on target gene expression when compared to CMT-U27 cells in MOCK control condition. However, qPCR results showed some significant downregulations of Wnt target genes, for example *Axin2* and *LEF1*. Furthermore, Western blot results showed a reduction of pSRC protein expression in the HER2 and HER3 silenced cells at 72 hours, indicating that silencing of HER2 or HER3 indeed influence phosphorylation of SRC, but that it takes some time before protein levels are affected by knockdown. However, fold changes of the significantly altered target genes were quite subtle, so drawing hard conclusions based on these results is heavy. In addition, the results of the Western blot were based on a single experiment, since we faced problems with succeeding of Western blot. Therefore, we cannot conclude that HER2 and HER3 silencing leads to decreased pSRC protein levels. Repetition of the experiment is necessary to confirm these only once obtained results.

Literature shows some contradicting results when focusing on the relationship between EGF receptors and the canonical Wnt pathway. Khalil *et al.* demonstrated a positive correlation between HER2 expression and nucleocytoplasmic β-catenin. (64) Also other studies showed a positive relationship between increased β-catenin levels and HER2 expression. (89) In contradiction, a study of Geyer *et al.* showed a negative correlation between HER2 expression and β-catenin levels. (90) Also other investigators demonstrated an inverse correlation between HER2 expression and β-catenin. (91)

So, repeating the experiments, with siRNAs which possibly induce higher knockdown efficiency, would be a recommendation to obtain more consistent results and more clarity about the possible roles of HER2 and HER3 in the activation of the canonical Wnt pathway.
Another recommendation could be to transfect the cells with both the HER2 and HER3 siRNA at the same time. It could be possible that silencing of only one of the two receptors does not induce strong effects. Both receptors depend on heterodimerization, since ligands are not able to bind HER2 and since HER3 has no intrinsic kinase activity. So both receptors collaborate closely. Therefore, it could be possible that only knockdown of both receptors results in effects.
More literature is available about the interaction of EGFR (HER1) and SRC, than about the interactions of HER2 and HER3 with SRC. (92)(93) Therefore, it is possible that EGFR and/or EGFR containing dimers play the major role in activating SRC, thereby stimulating the canonical Wnt pathway. Thus, knockdown of EGFR in CMT-U27 cells could also be a next step in the search for an explanation for the high canonical Wnt activity in the CMT-U27 cell line.

6. References

1. Silver IA. The anatomy of the mammary gland of the dog and cat. *J Small Anim Pract*. 1966 Nov;7(11):689–96. Available from: http://www.ncbi.nlm.nih.gov/pubmed/6009574

2. Sorenmo KU, Rasotto R, Zappulli V, Goldschmidt MH. Development, anatomy, histology, lymphatic drainage, clinical features, and cell differentiation markers of canine mammary gland neoplasms. *Vet Pathol*. 2011;48(1):85–97. doi: 10.1177/0300985810389480

3. Borena BM, Bussche L, Burvenich C, Duchateau L, Van de Walle GR. Mammary stem cell research in veterinary science: an update. *Stem Cells Dev*. 2013;22(12):1743–51. doi: 10.1089/scd.2012.0677

4. Brisken C, O'Malley B. Hormone action in the mammary gland. *Cold Spring Harb Perspect Biol*. 2010;2(12):1-15. doi: 10.1101/cshperspect.a003178

5. Peña L, Gama A, Goldschmidt MH, Abadie J, Benazzi C, Castagnaro M, et al. Canine mammary tumors: a review and consensus of standard guidelines on epithelial and myoepithelial phenotype markers, HER2, and hormone receptor assessment using immunohistochemistry. *Vet Pathol*. 2014;51(1):127–45. doi: 10.1177/0300985813509388

6. Sleeckx N, de Rooster H, Veldhuis Kroeze EJB, Van Ginneken C, Van Brantegem L. Canine mammary tumours, an overview. *Reprod Domest Anim*. 2011;46(6):1112–31. doi: 10.1111/j.1439-0531.2011.01816.x

7. Dyce K, Sack W, Wensing C. The Abdomen of the Dog and Cat-Mammary Glands. In: Dyce K, Sack W, Wensing C, eds. *Textbook of Veterinary Anatomy*. 4th ed. Saunders Elsevier; 2010. p. 434–5.

8. MacEwen EG. Spontaneous tumors in dogs and cats: models for the study of cancer biology and treatment. *Cancer Metastasis Rev*. 1990;9(2):125–36. Available from: http://www.ncbi.nlm.nih.gov/pubmed/2253312

9. Munson L, Moresco A. Comparative pathology of mammary gland cancers in domestic and wild animals. *Breast Dis*. 2007;28:7–21. Available from: http://www.ncbi.nlm.nih.gov/pubmed/18057539

10. Chiang K-C, Yeh C-N, Chung L-C, Feng T-H, Sun C-C, Chen M-F, et al. WNT-1 inducible signaling pathway protein-1 enhances growth and tumorigenesis in human breast cancer. *Sci Rep*. 2015;5:8686. doi: 10.1038/srep08686

11. Rabbani SA, Mazar AP. Evaluating distant metastases in breast cancer: from biology to outcomes. *Cancer Metastasis Rev*. 2007;26(3-4):663–74. doi: 10.1007/s10555-007-9085-8

12. Majchrzak K, Lo Re D, Gajewska M, Bulkowska M, Homa A, Pawłowski K, et al. Migrastatin analogues inhibit canine mammary cancer cell migration and invasion. *PLoS One*. 2013;8(10):1-13. doi: 10.1371/journal.pone.0076789

13. Liu D, Xiong H, Ellis AE, Northrup NC, Rodriguez CO, O'Regan RM, et al. Molecular homology and difference between spontaneous canine mammary cancer and human breast cancer. *Cancer Res*. 2014;74(18):5045–56. doi: 10.1158/0008-5472.CAN-14-0392

14. Sassi F, Benazzi C, Castellani G, Sarli G. Molecular-based tumour subtypes of canine mammary carcinomas assessed by immunohistochemistry. *BMC Vet Res*. 2010;6(5):1-9. doi: 10.1186/1746-6148-6-5

15. Gama A, Alves A, Schmitt F. Identification of molecular phenotypes in canine mammary carcinomas with clinical implications: application of the human classification. *Virchows Arch*. 2008;453(2):123–32. doi: 10.1007/s00428-008-0644-3

16. Engstrøm MJ, Opdahl S, Hagen AI, Romundstad PR, Akslen LA, Haugen OA, et al. Molecular subtypes, histopathological grade and survival in a historic cohort of breast cancer patients. *Breast Cancer Res Treat*. 2013;140(3):463–73. doi: 10.1007/s10549-013-2647-2

17. Im KS, Kim NH, Lim HY, Kim HW, Shin JI, Sur JH. Analysis of a new histological and molecular-based classification of canine mammary neoplasia. *Vet Pathol*. 2014;51(3):549–59. doi: 10.1177/0300985813498780

18. Foroni C, Broggini M, Generali D, Damia G. Epithelial-mesenchymal transition and breast cancer: role, molecular mechanisms and clinical impact. *Cancer Treat Rev*. 2012;38(6):689–97. doi: 10.1016/j.ctrv.2011.11.001

19. Radisky DC. Epithelial-mesenchymal transition. *J Cell Sci.* 2005;118(Pt 19):4325–6. doi: 10.1242/jcs.02552

20. Johansson J, Tabor V, Wikell A, Jalkanen S, Fuxe J. TGF-β1-Induced Epithelial-Mesenchymal Transition Promotes Monocyte/Macrophage Properties in Breast Cancer Cells. *Front Oncol*. 2015;5(3):1-9 doi: 10.3389/fonc.2015.00003

21. Li J, Zhou BP. Activation of β-catenin and Akt pathways by Twist are critical for the maintenance of EMT associated cancer stem cell-like characters. *BMC Cancer*. 2011;11(49):1-11. doi: 10.1186/1471-2407-11-49

22. Kotiyal S, Bhattacharya S. Breast cancer stem cells, EMT and therapeutic targets. *Biochem Biophys Res Commun*. 2014;453(1):112–6. doi: 10.1016/j.bbrc.2014.09.069

23. Takebe N, Warren RQ, Ivy SP. Breast cancer growth and metastasis: interplay between cancer stem cells, embryonic signaling pathways and epithelial-to-mesenchymal transition. *Breast Cancer Res*. 2011;13(3):211. doi: 10.1186/bcr2876

24. Hung T-H, Hsu S-C, Cheng C-Y, Choo K-B, Tseng C-P, Chen T-C, et al. Wnt5A regulates ABCB1 expression in multidrug-resistant cancer cells through activation of the non-canonical PKA/β-catenin pathway. *Oncotarget*. 2014;5(23):12273–90. Available from: http://www.pubmedcentral.nih.gov/articlerender.fcgi?artid=4322984&tool=pmcentrez&rendertype=abstract

25. Lindvall C, Bu W, Williams BO, Li Y. Wnt signaling, stem cells, and the cellular origin of breast cancer. *Stem Cell Rev*. 2007;3(2):157–68. doi: 10.007/s12015-007-0025-3

26. De A. Wnt/Ca2+ signaling pathway: a brief overview. *Acta Biochim Biophys Sin (Shanghai)*. 2011;43(10):745–56. doi: 10.1093/abbs/gmr079

27. Yu J, Virshup DM. Updating the Wnt pathways. *Biosci Rep*. 2014;34(5):593-607. doi: 10.1042/BSR20140119

28. King TD, Zhang W, Suto MJ, Li Y. Frizzled7 as an emerging target for cancer therapy. *Cell Signal*. 2012;24(4):846–51. doi: 10.1016/j.cellsig.2011.12.009

29. Komiya Y, Habas R. Wnt signal transduction pathways. *Organogenesis*. 2008;4(2):68–75. Available from: http://www.pubmedcentral.nih.gov/articlerender.fcgi?artid=2634250&tool=pmcentrez&rendertype=abstract

30. Janda CY, Waghray D, Levin AM, Thomas C, Garcia KC. Structural basis of Wnt recognition by Frizzled. *Science*. 2012;337(6090):59–64. doi: 10.1126/science.1222879

31. MacDonald BT, Tamai K, He X. Wnt/beta-catenin signaling: components, mechanisms, and diseases. *Dev Cell*. 2009;17(1):9–26. doi: 10.1016/j.devcel.2009.06.016

32. Widelitz R. Wnt signaling through canonical and non-canonical pathways: recent progress. *Growth Factors*. 2005;23(2):111–6. doi: 10.1080/08977190500125746

33. Zhao Z, Lu P, Zhang H, Xu H, Gao N, Li M, et al. Nestin positively regulates the Wnt/β-catenin pathway and the proliferation, survival and invasiveness of breast cancer stem cells. *Breast Cancer Res*. 2014;16(4):1-12. doi: 10.1186/s13058-014-0408-8

34. Boras-Granic K, Hamel PA. Wnt-signalling in the embryonic mammary gland. J *Mammary Gland Biol Neoplasia*. 2013;18(2):155–63. doi: 10.1007/s10911-013-9280-x

35. Xu J, Chen Y, Huo D, Khramtsov A, Khramtsova G, Zhang C, et al. β-catenin regulates c-Myc and CDKN1A expression in breast cancer cells. *Mol Carcinog*. 2015; doi: 10.1002/mc.22292

36. Micalizzi DS, Farabaugh SM, Ford HL. Epithelial-mesenchymal transition in cancer: parallels between normal development and tumor progression. *J Mammary Gland Biol Neoplasia*. 2010;15(2):117–34. doi: 10.1007/s10911-010-9178-9

37. Turashvili G, Bouchal J, Burkadze G, Kolar Z. Wnt signaling pathway in mammary gland development and carcinogenesis. *Pathobiology*. 2006;73(5):213–23. doi: 10.1159/000098207

38. Kohn AD, Moon RT. Wnt and calcium signaling: beta-catenin-independent pathways. *Cell Calcium*. 2005;38(3-4):439–46. doi: 10.1016/j.ceca.2005.06.022

39. Wang Y. Wnt/Planar cell polarity signaling: a new paradigm for cancer therapy. *Mol Cancer Ther*. 2009;8(8):2103–9. doi: 10.1158/1535-7163.MCT-09-0282

40. Loh YN, Hedditch EL, Baker LA, Jary E, Ward RL, Ford CE. The Wnt signalling pathway is upregulated in an in vitro model of acquired tamoxifen resistant breast cancer. *BMC Cancer*. 2013;13(174):1-9. doi: 10.1186/1471-2407-13-174

41. Wu Y, Ginther C, Kim J, Mosher N, Chung S, Slamon D, et al. Expression of Wnt3 activates Wnt/β-catenin pathway and promotes EMT-like phenotype in trastuzumab-resistant HER2-overexpressing breast cancer cells. *Mol Cancer Res*. 2012;10(12):1597–606. doi: 10.1158/1541-7786.MCR-12-0155-T

42. Qiao L, Liang Y, Mira RR, Lu Y, Gu J, Zheng Q. Mammalian target of rapamycin (mTOR) inhibitors and combined chemotherapy in breast cancer: a meta-analysis of randomized controlled trials. *Int J Clin Exp Med*. 2014;7(10):3333–43. Available from: http://www.pubmedcentral.nih.gov/articlerender.fcgi?artid=4238547&tool=pmcentrez&rendertype=abstract

43. Tokunaga E, Hisamatsu Y, Tanaka K, Yamashita N, Saeki H, Oki E, et al. Molecular mechanisms regulating the hormone sensitivity of breast cancer. *Cancer Sci*. 2014;105(11):1377–83. doi: 10.1111/cas.12521

44. Zhao M, Ramaswamy B. Mechanisms and therapeutic advances in the management of endocrine-resistant breast cancer. *World J Clin Oncol*. 2014;5(3):248–62. doi: 10.5306/wjco.v5.i3.248

45. Ciruelos Gil EM. Targeting the PI3K/AKT/mTOR pathway in estrogen receptor-positive breast cancer. *Cancer Treat Rev*. 2014;40(7):862–71. doi: 10.1016/j.ctrv.2014.03.004

46. Paplomata E, O'Regan R. The PI3K/AKT/mTOR pathway in breast cancer: targets, trials and biomarkers. *Ther Adv Med Oncol*. 2014;6(4):154–66. doi: 10.1177/1758834014530023

47. O'Regan R, Hawk NN. mTOR inhibition in breast cancer: unraveling the complex mechanisms of mTOR signal transduction and its clinical implications in therapy. *Expert Opin Ther Targets*. 2011;15(7):859–72. doi: 10.1517/14728222.2011.575362

48. Phin S, Moore MW, Cotter PD. Genomic Rearrangements of PTEN in Prostate Cancer. *Front Oncol* . 2013;3(240):1-9. doi: 10.3389/fonc.2013.00240

49. Nagaraj G, Ma C. Revisiting the estrogen receptor pathway and its role in endocrine therapy for postmenopausal women with estrogen receptor-positive metastatic breast cancer. *Breast Cancer Res Treat*. 2015;150(2):231–42. doi: 10.1007/s10549-015-3316-4

50. Chia S, Gandhi S, Joy AA, Edwards S, Gorr M, Hopkins S, et al. Novel agents and associated toxicities of inhibitors of the pi3k/Akt/mtor pathway for the treatment of breast cancer. *Curr Oncol*. 2015;22(1):33–48. doi: 10.3747/co.22.2393

51. Arena F. Clinical implications of recent studies using mTOR inhibitors to treat advanced hormone receptor-positive breast cancer. *Cancer Manag Res*. 2014;4(6):389–95. doi: 10.2147/CMAR.S56802

52. Gracanin A, Timmermans-Sprang EPM, van Wolferen ME, Rao NAS, Grizelj J, Vince S, et al. Ligand-independent canonical Wnt activity in canine mammary tumor cell lines associated with aberrant LEF1 expression. *PLoS One*. 2014;9(6):1-12. doi: 10.1371/journal.pone.0098698

53. Timmermans-Sprang EPM, Gracanin A, Mol JA. High basal Wnt signaling is further induced by PI3K/mTor inhibition but sensitive to cSRC inhibition in mammary carcinoma cell lines with HER2/3 overexpression. *BMC Cancer*. 2015;15(545):1-12. doi: 10.1186/s12885-015-1544-y

54. Elsberger B. Translational evidence on the role of Src kinase and activated Src kinase in invasive breast cancer. *Crit Rev Oncol Hematol*. 2014;89(3):343–51. doi: 10.1016/j.critrevonc.2013.12.009

55. Formisano L, Nappi L, Rosa R, Marciano R, D'Amato C, D'Amato V, et al. Epidermal growth factor-receptor activation modulates Src-dependent resistance to lapatinib in breast cancer models. *Breast Cancer Res*. 2014;16(3):1-15. doi: 10.1186/bcr3650

56. Parsons SJ, Parsons JT. Src family kinases, key regulators of signal transduction. *Oncogene*. 2004;23(48):7906–9. doi: 10.1038/sj.onc.1208160

57. Yokoyama N, Malbon CC. Dishevelled-2 docks and activates Src in a Wnt-dependent manner. *J Cell Sci*. 2009;122(Pt 24):4439–51. doi: 10.1242/jcs.051847

58. Zhang S, Yu D. Targeting Src family kinases in anti-cancer therapies: turning promise into triumph. *Trends Pharmacol Sci*. 2012;33(3):122–8. doi: 10.1016/j.tips.2011.11.002

59. Peiró G, Ortiz-Martínez F, Gallardo A, Pérez-Balaguer A, Sánchez-Payá J, Ponce JJ, et al. Src, a potential target for overcoming trastuzumab resistance in HER2-positive breast carcinoma. *Br J Cancer*. 2014;111(4):689–95. doi: 10.1038/bjc.2014.327

60. Bain J, Plater L, Elliott M, Shpiro N, Hastie CJ, McLauchlan H, et al. The selectivity of protein kinase inhibitors: a further update. *Biochem J*. 2007;408(3):297–315. doi: 10.1042/BJ20070797

61. Bain J, McLauchlan H, Elliott M, Cohen P. The specificities of protein kinase inhibitors: an update. *Biochem J*. 2003;371(Pt 1):199–204. doi: 10.1042/BJ20021535

62. Kim LC, Song L, Haura EB. Src kinases as therapeutic targets for cancer. *Nat Rev Clin Oncol*. 2009;6(10):587–95. doi: 10.1038/nrclinonc.2009.129

63. Mao Z, Liu Z, Chen L, Yang J, Zhao B, Jung YM, et al. Predictive value of the surface-enhanced resonance Raman scattering-based MTT assay: a rapid and ultrasensitive method for cell viability in situ. *Anal Chem*. 2013;85(15):7361–8. doi: 10.1021/ac401254s

64. Khalil S, Tan GA, Giri DD, Zhou XK, Howe LR. Activation status of Wnt/ß-catenin signaling in normal and neoplastic breast tissues: relationship to HER2/neu expression in human and mouse. *PLoS One*. 2012;7(3):e33421. doi: 10.1371/journal.pone.0033421

65. Liang C-C, Park AY, Guan J-L. In vitro scratch assay: a convenient and inexpensive method for analysis of cell migration in vitro. *Nat Protoc*. 2007;2(2):329–33. doi: 10.1038/nprot.2007.30

66. Doleschall M, Mayer B, Cervenak J, Cervenak L, Kacskovics I. Cloning, expression and characterization of the bovine p65 subunit of NFkappaB. *Dev Comp Immunol*. 2007;31(9):945–61. doi: 10.1016/j.dci.2006.12.007

67. Xiang Lu RF. Inhibition of epithelial to mesenchymal transition in metastatic breast carcinoma cells by c-Src suppression. *Acta Biochim Biophys Sin*. 2010;42(7):496–501. doi: 10.1093/abbs/gmq043.

68. Dar AA, Belkhiri A, El-Rifai W. The aurora kinase A regulates GSK-3beta in gastric cancer cells. *Oncogene*. 2009;28(6):866–75. doi: 10.1038/onc.2008.434

69. Jia L, Lee HS, Wu CF, Kundu J, Park SG, Kim RN, et al. SMAD4 suppresses AURKA-induced metastatic phenotypes via degradation of AURKA in a TGFβ-independent manner. *Mol Cancer Res*. 2014;12(12):1779–95. doi: 10.1158/1541-7786.MCR-14-0191

70. Yang H, He L, Kruk P, Nicosia S V, Cheng JQ. Aurora-A induces cell survival and chemoresistance by activation of Akt through a p53-dependent manner in ovarian cancer cells. *Int J Cancer*. 2006;119(10):2304–12. doi: 10.1002/ijc.22154

71. Gao C, Chen Y-G. Dishevelled: The hub of Wnt signaling. *Cell Signal*. 2010;22(5):717–27. doi: 10.1016/j.cellsig.2009.11.021

72. Couffinhal T, Dufourcq P, Duplàa C. Beta-catenin nuclear activation: common pathway between Wnt and growth factor signaling in vascular smooth muscle cell proliferation? *Circ Res*. 2006;99(12):1287–9. doi: 10.1161/01.RES.0000253139.82251.31

73. Karni R, Gus Y, Dor Y, Meyuhas O, Levitzki A. Active Src elevates the expression of beta-catenin by enhancement of cap-dependent translation. *Mol Cell Biol*. 2005;25(12):5031–9. doi: 10.1128/MCB.25.12.5031-5039.2005

74. Fonte C, Grenier J, Trousson A, Chauchereau A, Lahuna O, Baulieu E-E, et al. Involvement of {beta}-catenin and unusual behavior of CBP and p300 in glucocorticosteroid signaling in Schwann cells. *Proc Natl Acad Sci U S A*. 2005;102(40):14260–5. doi: 10.1073/pnas.0506930102

75. Tong Z, Li M, Wang W, Mo P, Yu L, Liu K, et al. Steroid Receptor Coactivator 1 Promotes Human Hepatocellular Carcinoma Progression by Enhancing Wnt/β-Catenin Signaling. *J Biol Chem*. 2015;290(30):18596–608. doi: 10.1074/jbc.M115.640490

76. Tania M, Khan MA, Fu J. Epithelial to mesenchymal transition inducing transcription factors and metastatic cancer. *Tumour Biol*. 2014;35(8):7335–42. doi: 10.1007/s13277-014-2163-y

77. Serra V, Scaltriti M, Prudkin L, Eichhorn PJA, Ibrahim YH, Chandarlapaty S, et al. PI3K inhibition results in enhanced HER signaling and acquired ERK dependency in HER2-overexpressing breast cancer. *Oncogene*. 2011;30(22):2547–57. doi: 10.1038/onc.2010.626

78. Stern DF. ERBB3/HER3 and ERBB2/HER2 duet in mammary development and breast cancer. *J Mammary Gland Biol Neoplasia*. 2008;13(2):215–23. doi: 10.1007/s10911-008-9083-7

79. Aceto N, Duss S, MacDonald G, Meyer DS, Roloff T-C, Hynes NE, et al. Co-expression of HER2 and HER3 receptor tyrosine kinases enhances invasion of breast cells via stimulation of interleukin-8 autocrine secretion. *Breast Cancer Res*. 2012;14(5):1-11. doi: 10.1186/bcr3329

80. Mocellin S, Provenzano M. RNA interference: learning gene knock-down from cell physiology. *J Transl Med*. 2004;2(1):1-6. doi: 10.1186/1479-5876-2-39

81. Livak KJ, Schmittgen TD. Analysis of relative gene expression data using real-time quantitative PCR and the 2(-Delta Delta C(T)) Method. *Method*. 2001;25(4):402–8. doi: 10.1006/meth.2001.1262

82. Glaysher S, Bolton LM, Johnson P, Torrance C, Cree IA. Activity of EGFR, mTOR and PI3K inhibitors in an isogenic breast cell line model. *BMC Res Notes*. 2014;7(397):1-7. doi: 10.1186/1756-0500-7-397

83. Wilson-Edell KA, Yevtushenko MA, Rothschild DE, Rogers AN, Benz CC. mTORC1/C2 and pan-HDAC inhibitors synergistically impair breast cancer growth by convergent AKT and polysome inhibiting mechanisms. *Breast Cancer Res Treat*. 2014;144(2):287–98. doi: 10.1007/s10549-014-2877-y

84. Jho E, Zhang T, Domon C, Joo C-K, Freund J-N, Costantini F. Wnt/beta-catenin/Tcf signaling induces the transcription of Axin2, a negative regulator of the signaling pathway. *Mol Cell Biol*. 2002;22(4):1172–83. doi: 10.1128/MCB.22.4.1172–1183.2002

85. Qian J, Zou Y, Rahman JSM, Lu B, Massion PP. Synergy between phosphatidylinositol 3-kinase/Akt pathway and Bcl-xL in the control of apoptosis in adenocarcinoma cells of the lung. *Mol Cancer Ther*. 2009;8(1):101–9. doi: 10.1158/1535-7163.MCT-08-0973

86. Fuentealba RA, Farias G, Scheu J, Bronfman M, Marzolo MP, Inestrosa NC. Signal transduction during amyloid-beta-peptide neurotoxicity: role in Alzheimer disease. *Brain Res Rev*. 2004;47(1-3):275–89. doi: 10.1016/j.brainresrev.2004.07.018

87. Filali M, Cheng N, Abbott D, Leontiev V, Engelhardt JF. Wnt-3A/beta-catenin signaling induces transcription from the LEF-1 promoter. *J Biol Chem*. 2002;277(36):33398–410. doi: 10.1074/jbc.M107977200

88. Di Liddo R, Bertalot T, Schuster A, Schrenk S, Tasso A, Zanusso I, et al. Anti-inflammatory activity of Wnt signaling in enteric nervous system: in vitro preliminary evidences in rat primary cultures. *J Neuroinflammation*. 2015;12:23. doi: 10.1186/s12974-015-0248-1

89. López-Knowles E, Zardawi SJ, McNeil CM, Millar EKA, Crea P, Musgrove EA, et al. Cytoplasmic localization of beta-catenin is a marker of poor outcome in breast cancer patients. *Cancer Epidemiol Biomarkers Prev*. 2010;19(1):301–9. doi: 10.1158/1055-9965.EPI-09-0741

90. Geyer FC, Lacroix-Triki M, Savage K, Arnedos M, Lambros MB, MacKay A, et al. β-Catenin pathway activation in breast cancer is associated with triple-negative phenotype but not with CTNNB1 mutation. *Mod Pathol*. 2011;24(2):209–31. doi: 10.1038/modpathol.2010.205

91. Khramtsov AI, Khramtsova GF, Tretiakova M, Huo D, Olopade OI, Goss KH. Wnt/beta-catenin pathway activation is enriched in basal-like breast cancers and predicts poor outcome. *Am J Pathol*. 2010;176(6):2911–20. doi: 10.2353/ajpath.2010.091125

92. Paul I, Bhattacharya S, Chatterjee A, Ghosh MK. Current Understanding on EGFR and Wnt/β-Catenin Signaling in Glioma and Their Possible Crosstalk. *Genes Cancer*. 2013;4(11-12):427–46. doi: 10.1177/1947601913503341

93. Bogdan S, Klämbt C. Epidermal growth factor receptor signaling. *Curr Biol*. 2001;11(8):R292–5. doi: 10.1016/S0960-9822(01)00167-1

7. Acknowledgements

First of all I would like to thank my supervisors, Ing. Elpetra Timmermans-Sprang and Dr. Ir. Jan Mol:

Elpetra, thank you very much for all the assistance on the lab during this year. When I came to the lab in September 2014, all laboratory techniques were unknown for me. Now, a year later, I am comfortable with several laboratory techniques. Thank you very much for that! Also thanks for your help in analyzing the results, ideas, suggestions and enthusiasm throughout this year.

Jan, thank you for your wise input and suggestions during the meetings. Your knowledge about so many subjects is impressive!

I would also like to thank Adri Slob, Monique van Wolferen and Loes Oosterhoff for their guidance at the lab.

Karin, Margriet and Stijn, thank you for the nice atmosphere in our workroom! Also thanks for listening to frustrations about failed experiments some times.

Last but not least, I would like to thank the MOC research commission for giving me the opportunity to participate in the Honours Programme.

8. Appendices

Appendix 8A: List of abbreviations

Abbreviation	Description
AKT	Protein kinase B
APC	Adenomatosis polyposis coli
Axin2	Conductin protein/axil protein/Axis inhibition protein 2
B2M	Beta-2-microglobulin
BCL2	B-cell CLL/lymphoma 2
BCSC	Breast cancer stem cell
β-TrCP	B-transducin repeat containing protein
BLAST	Basic Local Alignment Search Tool
BSA	Bovine Serum Albumin
CAMKII	Ca^{2+}/calmodulin dependent protein kinase II
CK1α	Casein kinase 1α
cMET	Met proto-oncogene, also known as hepatocyte growth factor receptor
CMTs	Canine mammary tumors
cMYC	v-myc myelocytomatosis viral oncogene homolog
CRD	Cysteine-rich domain
CtBP	C-terminal binding protein
DMSO	Dimethyl sulfoxide
DVL	Dishevelled protein
ECM	Extracellular matrix
EFG	Epidermal growth factor
EGFR/HER1	Human epidermal growth factor receptor 1
EMT	Epithelial mesenchymal transition
FCS	Fetal Calf Serum
F	Forward primer
GAPDH	Glyceraldehyde-3-phosphate dehydrogenase
G protein	Guanosine triphosphate binding protein
GSK-3β	Glycogen synthase kinase 3β
GUSB	Glucuronidase beta
HER2	Human epidermal growth factor receptor 2
HER3	Human epidermal growth factor receptor 3
HER4	Human epidermal growth factor receptor 4
HMBS	Hydroxymethylbilane synthase
HNRPH	Heterogeneous nuclear ribonucleoprotein H
HPRT	Hypoxanthine phosphoribosyltransferase 1
HSP90a	Heat shock protein 90a
IC50-value	Concentration of compound which induces 50% cell death
ID1	Inhibitor of DNA binding 1, dominant negative helix-loop-helix protein
ID2	Inhibitor of DNA binding 2, dominant negative helix-loop-helix protein
IGF1-R	Insulin-like growth factor receptor 1
JNK	c-jun-N-terminal kinase
kDa	Kilodalton
LEF1	Lymphoid enhancer binding factor 1
LRP5/6	Low-density-lipoprotein-related protein5/6

MET	Mesenchymal epithelial transition
milliQ	DNASe and RNAse free water
mTOR	Mammalian target of rapamycin
MTT	[3- (4,5-Dimethyl-2-thiazolyl)-2,5-diphenyl-2H-tetrazolium bromide]
µ	Micro
MUC1	Mucin 1, cell surface associated
n	Nano
NCBI	National Center for Biotechnology Information
NCOA3	Nuclear receptor coactivator 3
NRG1	Neuregulin 1
OVX	Ovari(ohyster)ectomy
PCP pathway	Planar Cell Polarity pathway
PGR	Progesterone receptor
PI3K	Phosphatidylinositol 3-kinase
PIP_2	Phosphatidylinositol 4,5 biphosphate
PIP_3	Phosphatidylinositol 3,4,4-triphosphate
PKC	Protein kinase C
PP2A	Protein phosphatase 2A
PTEN	Phosphatase and tensin homolog
qPCR	Real-time quantitative polymerase chain reaction
RAC1	Ras-related C3 botulinum toxin substrate 1
RAC1B	Ras-related C3 botulinum toxin substrate 1B
R	Reverse primer
RISC	RNA-inducing silencing complex
ROCK	Rho-associated kinase
RPL8	Ribosomal protein L8
RPL13	Ribosomal protein L13
RPS5	Ribosomal protein S5
RPS19	Ribosomal protein S19
RTKs	Receptor tyrosine kinases
SDHA	Succinate dehydrogenase complex, subunit A, flavoprotein (Fp)
SEM	Standard error of the mean
SFKs	SRC family of protein kinases
siRNA	Small interfering RNA, a mechanism whereby the expression of a certain gene is silenced
SLUG	Snail homolog 2, also known as SNAI2
SRC	Proto-oncogene SRC, derived from the word Sarcoma
SRPR	Signal recognition particle receptor
T_a	Annealing temperature
TBP	TATA box binding protein
TCF	Transcription factor
TGFα	Transforming growth factor alpha
TNBC	Triple negative breast cancer
TNFα	Tumor necrosis factor alpha
WHO	World Health Orgaization
YWHAZ	Tyrosine 3-monooxygenase/tryptophan 5-monooxygease activation protein, zeta polypeptide

Appendix 8B: Primers used for reference genes

OMIM	Symbol	Sequence (5'→ 3')	T_a	Product length (bp)	Accession number
B2M	**B2M**	**F:** TCCTCATCCTCCTCGCT **R:** TTCTCTGCTGGGTGTCG	62	85	AB745507
GAPDH	**GAPDH**	**F:** TGTCCCCACCCCCAATGTATC **R:** CTCCGATGCCTGCTTCACTACCTT	58	100	NM_001003142
GUSB	**GUSB**	**F:** AGACGCTTCCAAGTACCCC **R:** AGGTGTGGTGTAGAGGAGCAC	62	103	NM_001003191
HMBS	**HMBS**	**F:** TCACCATCGGAGCCATCT **R:** GTTCCCACCACGCTCTTCT	61	112	XM_546491
HNRNPH2	**HNRPH**	**F:** CTCACTATGATCCACCACG **R:** TAGCCTCCATAACCTCCAC	61,2	151	XM_538576
HPRT1	**HPRT**	**F:** AGCTTGCTGGTGAAAAGGAC **R:** TTATAGTCAAGGGCATATCC	57	104	NM_001003357
RPL8	**RPL8**	**F:** CCATGAATCCTGTGGAGC **R:** GTAGAGGGTTTGCCGATG	55	64	XM_532360
RPL13	**RPL13**	**F:** GCCGGAAGGTTGTAGTCGT **R:** GGAGGAAGGCCAGGTAATTC	61	87	XM_003432726
RPS5	**RPS5**	**F:** TCACTGGTGAGAACCCCCT **R:** CCTGATTCACACGGCGTAG	62,5	141	XM_533568
RPS19	**RPS19**	**F:** CCTTCCTCAAAAAGTCTGGG **R:** GTTCTCATCGTAGGGAGCAAG	62	95	XM_533657
SDHA	**SDHA**	**F:** GCCTTGGATCTCTTGATGGA **R:** TTCTTGGCTCTTATGCGATG	61	92	DQ402985
SRPR	**SRPR**	**F:** GCTTCAGGATCTGGACTGC **R:** GTTCCCTTGGTAGCACTGG	61,2	81	XM_546411
TBP	**TBP**	**F:** CTATTTCTTGGTGTGCATGAGG **R:** CCTCGGCATTCAGTCTTTTC	57	96	XM_849432
YWHAZ	**YWHAZ**	**F:** CGAAGTTGCTGCTGGTGA **R:** TTGCATTTCCTTTTTGCTGA	58	96	XM_843951

Appendix 8C: Primers used for target genes

OMIM	Symbol	Sequence (5'→ 3')	T_a	Product length (bp)	Accession number	Mean Ct-value Control
AXIN2	**Axin2**	**F:** GGACAAATGCGTGGATACCT **R:** TGCTTGGAGACAATGCTGTT	60	128	XM_54802	28.13
CTNNB1	**β-Catenin**	**F:** ATGGGTAGGGCAAATCAGTAAGAGGT **R:** AAGCATCGTATCACAGCAGGTTAC	64	106	XM_005634157.1	20.90
BNIPL	**BCL2**	**F:** TGGAGAGCGTCAACCGGGAGATGT **R:** AGGTGTGCAGATGCCGGTTCAGGT	62	87	AY_509563.1	27.14
MET	**cMET**	**F:** TGTGCTGTGAAATCCCTGAATAGAATC **R:** CCAAGAGTGAGAGTACGTTTGGATGAC	56	159	NM_001002963.1	28.58
MYC	**cMYC**	**F:** GCCGGCGCCCAGCGAGGATA **R:** GCGACTGCGACGTAGGAGGGCGAGC	61	108	NM_001003246	27.89
CCDN1	**CyclinD1**	**F:** GCCTCGAAGATGAAGGAGAC **R:** CAGTTTGTTCACCAGGAGCA	60	117	NM_001005757.1	22.28
CDH1	**E-Cadherin**	**F:** CAGGAAGCTCTCCACCAGAG **R:** CTGGGAAATGTGAGCACCTC	58	105	NM_001287125.1	23.42
ERBB1	**EGFR**	**F:** CTGGAGCATTCGGCA **R:** TGGCTTTGGGAGACG	53	107	XM_533073	27.03
ERBB2	**HER2**	**F:** CGTGCTGGACAATGGAGACC **R:** CCGCTGAATCAAGACCCCTC	64	51	AB008451	27.33
ERBB3	**HER3**	**F:** TAGTGGTGAAGGACAACGGCAG **R:** GGTCTTGGTCAATGTCTGGCAG	70	103	XM_538226	23.30
ERBB4	**HER4**	**F:** CAGTTCTTGTGTGCGTGCCTG **R:** ATGATCCTGTGCCGATGCC	64		XM_545629	29.16
HSP90AA1	**HSP90a**	**F:** CTTGACCGATCCCAGTAAGC **R:** TATTGATCAGGTCGGCCTTC	59	127	XR_134513.2	20.84
ID1	**ID1**	**F:** CTCAACGGCGAGATCAG **R:** GAGCACGGGTTCTTCTC	59,5	135	XM_847117.2	22.53
ID2	**ID2**	**F:** GCTGAATAAATGGTGTTCGTG **R:** GTTGTTCTCCTTGTGAAATGG	60,5	114	XR_134413.1	21.65
TCF7L3	**LEF1**	**F:** AGACATCCTCCAGCTCCTGA **R:** GATGGATAGGGTTGCCTGAA	60	137	XP_863334.2	25.09

MUC1	**MUC1**	**F:** CTATGAGGAGGTTTCTGCAG **R:** GAACACAGTTGAGAGGAGAG	62	172	NM_001194977	29.27
NCOA3	**NCOA3**	**F:** ATGCGGCCTGGTGAGATT **R:** TAAGAAGTGGCCTATTTTGAGTCC	67,1	141	ENSCAFT00000017243	24.85
NRG1	**NRG1**	**F:** CATCGCCCTGCTTGTGGTC **R:** GTGGTGAGGCCCGTTTGCTATG	67		NC_006598.3	32.27
PGR	**PGR**	**F:** CAATGGAAGGGCAGCATAAC **R:** CAGCACTTTCTAAGGCGACA	102	57	NM_001003074.1	29.24
RAC1	**RAC1**	**F:** TCCCTTATCCTATCCGCAAA **R:** ATGATAGGGGTGTTGGGACA	58	128	NM_001003274.2	21.55
RAC1B	**RAC1B**	**F:** TGGGATACAGCTGGACAAGA **R:** CTTGTCTTTGCCCCTGGAG	58	108	JN_182651.1	24.69
SNAI2	**SLUG**	**F:** CTTCACTCCGACTCCAAACG **R:** TGGATTTTGTGCTCTTGCAG	60	147	XM_005637933.1	29.08
SRC	**SRC**	**F:** CATTGGGAAGGGGGAGTTTGGAGA **R:** TGCCGAAGTTGCGTCATCACAGAG	66		XM_005638625.1	25.83
TGFA	**TGFα**	**F:** CCGCCTTGGTGGTGGTCTCC **R:** AGGGCGCTGGGCTTCTCTGT	61	83	NM_001003244.4	30.87
TNFA	**TNFα**	**F:** CCCCGGGCTCCAGAAGGTG **R:** GCAGCAGGCAGAAGAGTGTGGTG	65		AB_819629.1	37.33

Appendix 8D: geNorm Data Analysis Results

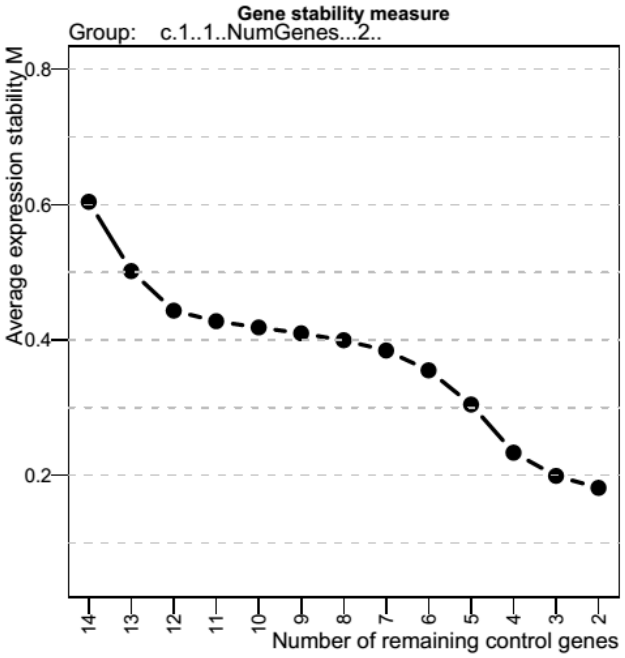

Figure 18. Stability of reference genes.

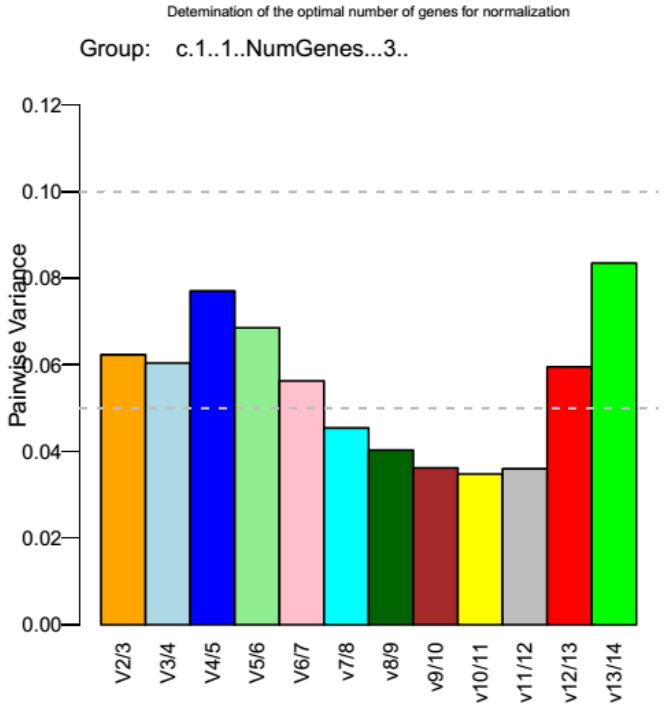

"Rank"	"1"	"All"
"1"	1	"RPS5"
"2"	1	"RPS19"
"3"	2	"RPL8"
"4"	3	"RPL13"
"5"	4	"SDHA"
"6"	5	"HNRPH"
"7"	6	"YWHAZ"
"8"	7	"TBP"
"9"	8	"SRPR"
"10"	9	"GUSB"
"11"	10	"HMBS"
"12"	11	"GAPDH"
"13"	12	"B2MG"
"14"	13	"HPRT"

Figure 19. Optimal number of genes for the lowest variance.

Appendix 8E: qPCR results

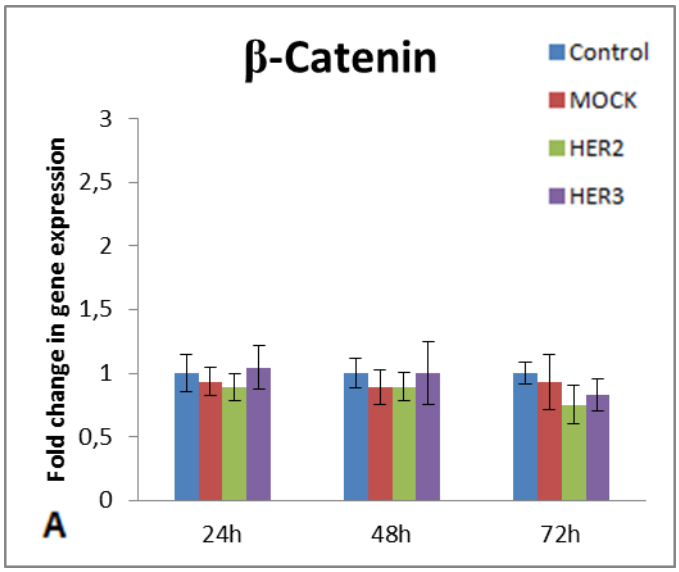

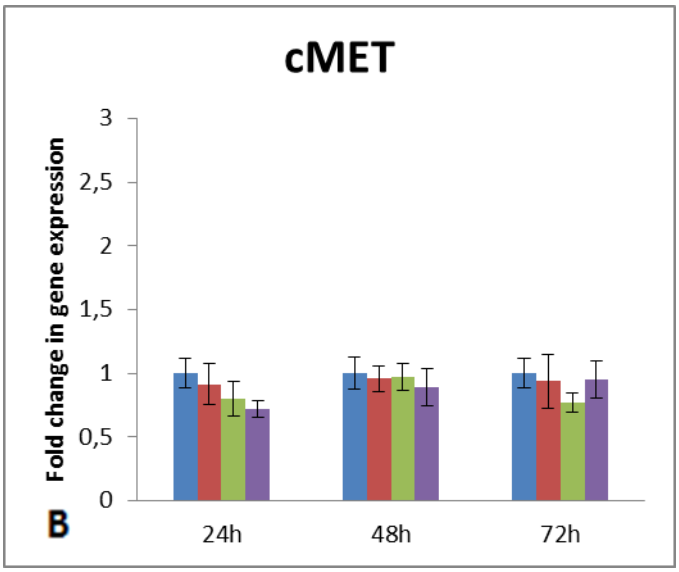

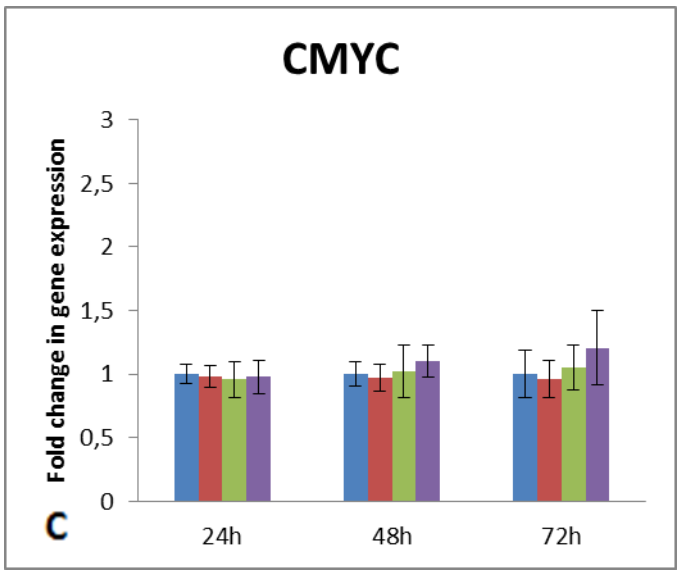

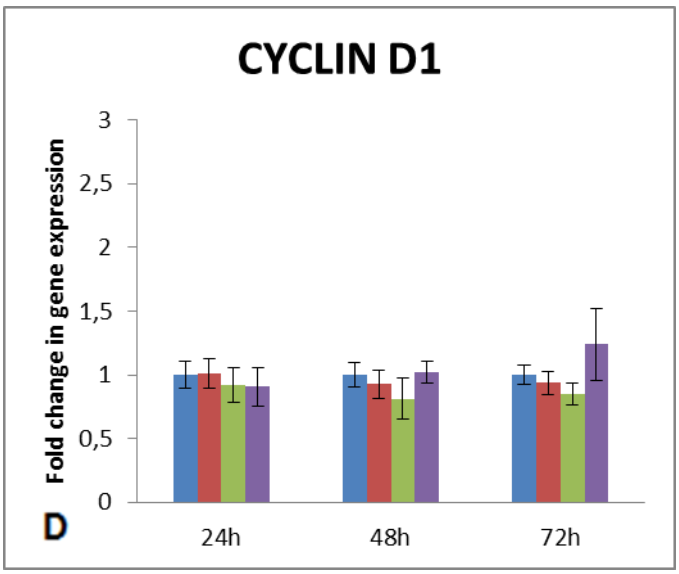

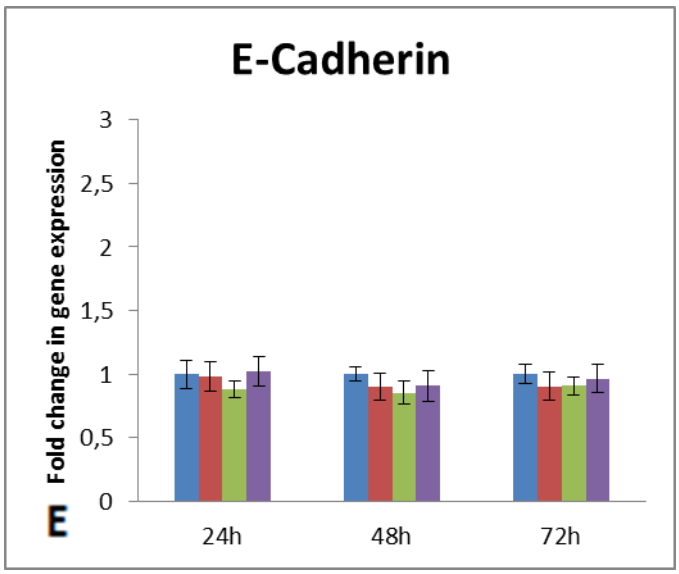

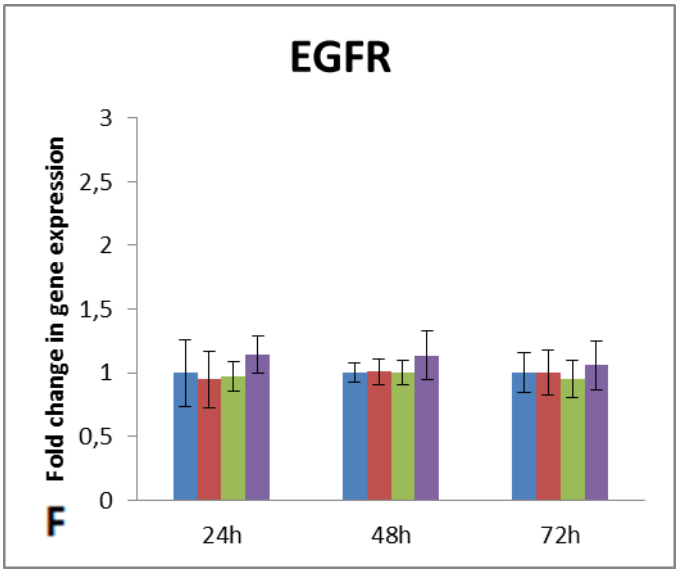
EGFR
Fold change in gene expression
3
2,5
2
1,5
1
0,5
0
24h
48h
72h
F

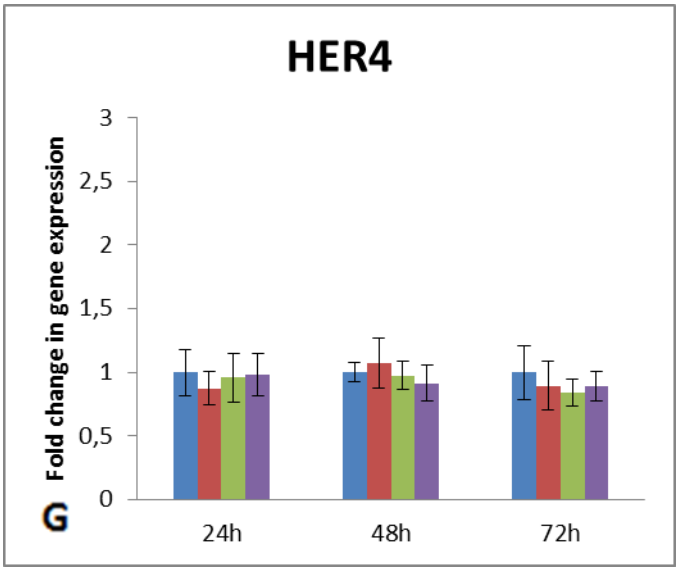
HER4
Fold change in gene expression
3
2,5
2
1,5
1
0,5
0
24h
48h
72h
G

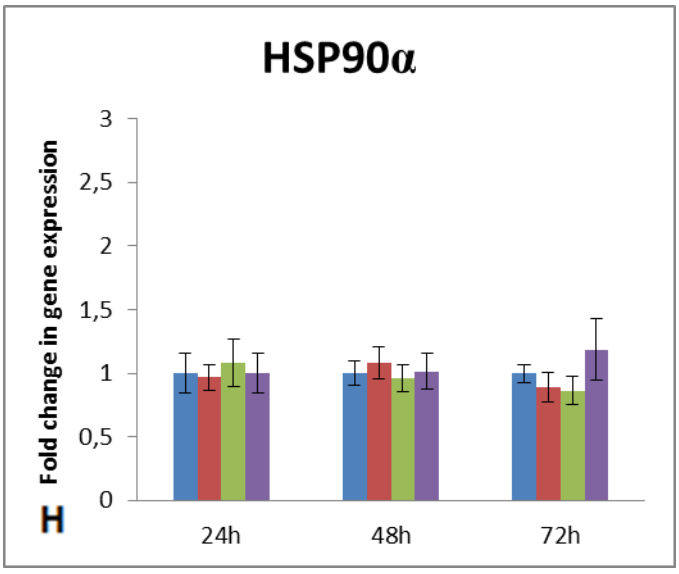
HSP90α
Fold change in gene expression
3
2,5
2
1,5
1
0,5
0
24h
48h
72h
H

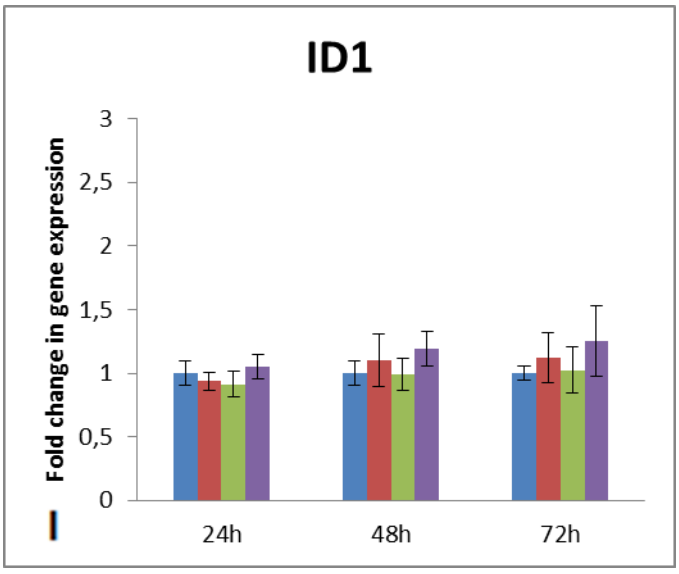
ID1
Fold change in gene expression
3
2,5
2
1,5
1
0,5
0
24h
48h
72h
I

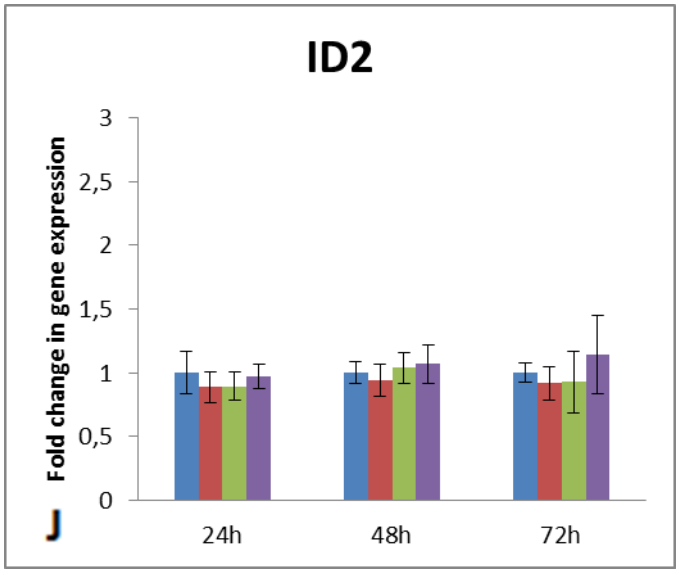
ID2
Fold change in gene expression
3
2,5
2
1,5
1
0,5
0
24h
48h
72h
J

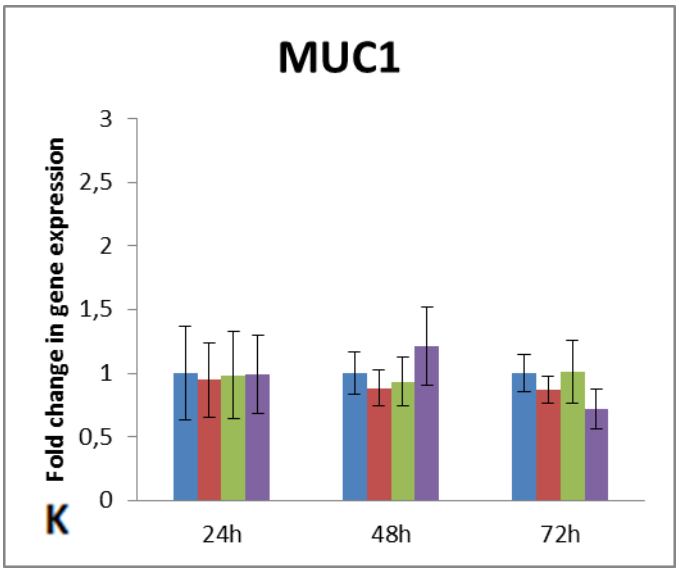
MUC1
Fold change in gene expression
3
2,5
2
1,5
1
0,5
0
24h
48h
72h
K

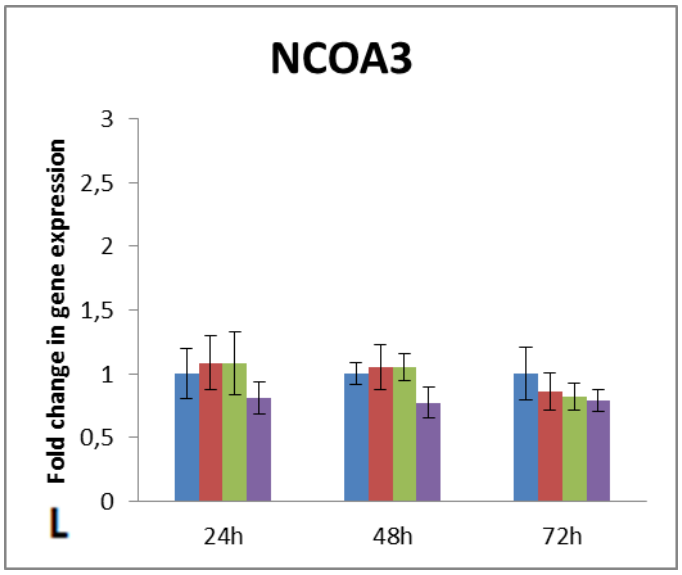
NCOA3
Fold change in gene expression
3
2,5
2
1,5
1
0,5
0
24h
48h
72h
L

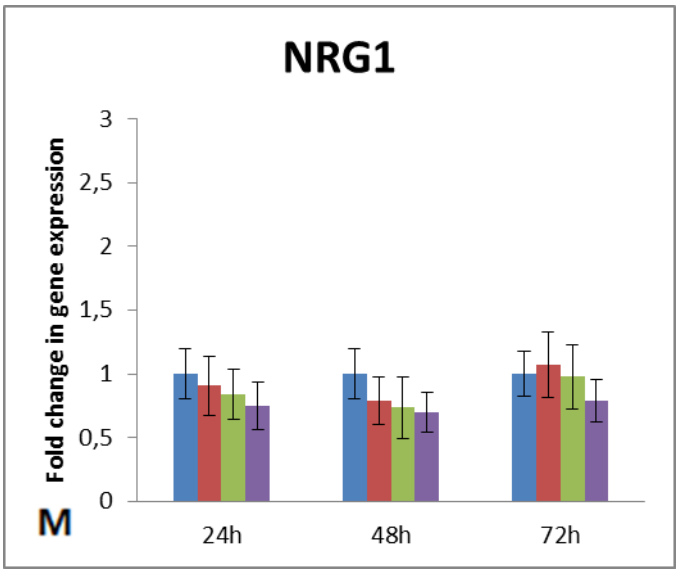
NRG1
Fold change in gene expression
3
2,5
2
1,5
1
0,5
0
24h
48h
72h
M

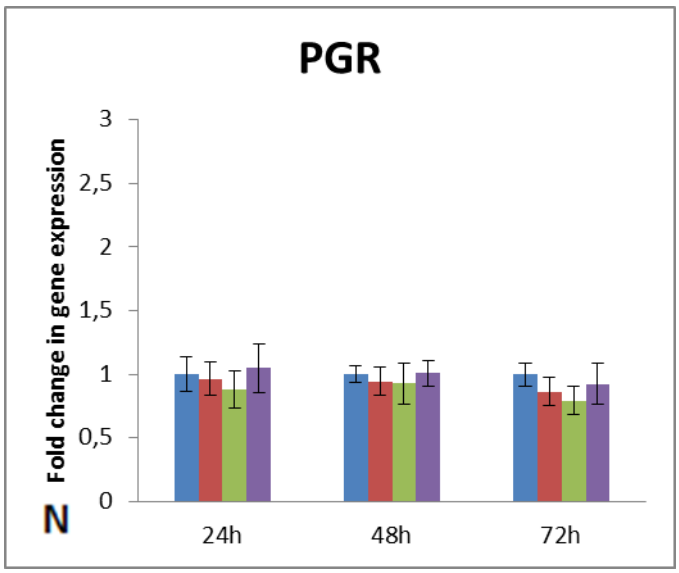
PGR
Fold change in gene expression
3
2,5
2
1,5
1
0,5
0
24h
48h
72h
N

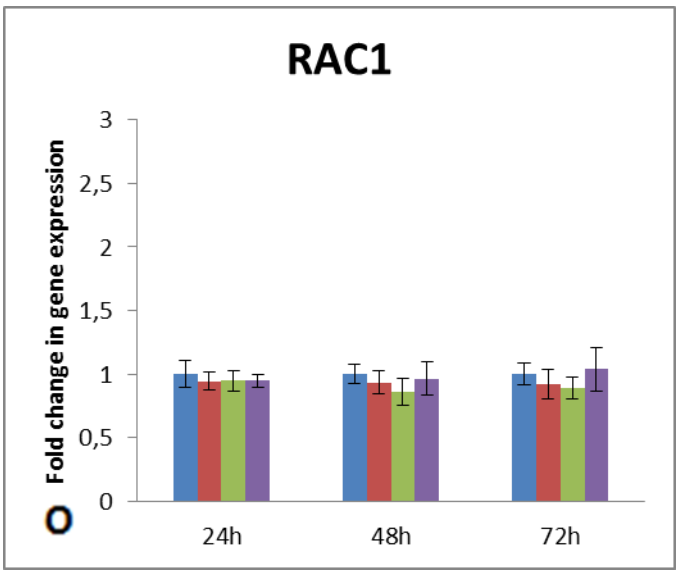
RAC1
Fold change in gene expression
3
2,5
2
1,5
1
0,5
0
24h
48h
72h
O

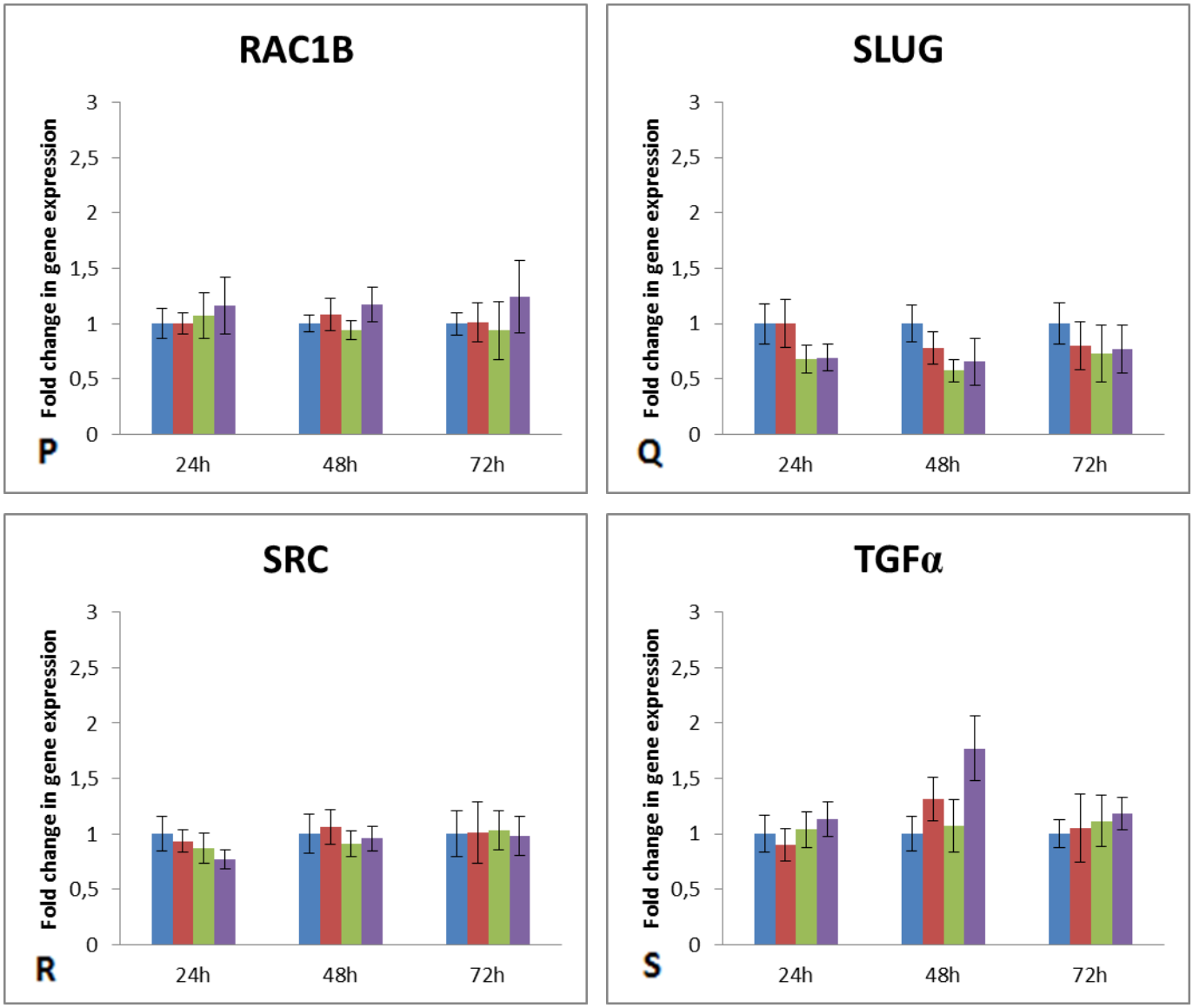

Figure 20. Gene expression of target genes in CMT-U27 cell line in control conditions (control and MOCK) and after silencing of HER2 and HER3. The cell line was grown for 24, 48 and 72 hours in the presence of MOCK, HER2 or HER3 siRNA. After incubation RNA was isolated and the relative expression of several target genes was measured by quantitative RT-PCR: β-Catenin (**A**), cMET (**B**), cMYC (**C**), CyclinD1 (**D**), E-Cadherin (**E**), EGFR (**F**), HER4 (**G**), HSP90α (**H**), ID1 (**I**), ID2 (**J**), MUC1 (**K**), NCOA3 (**L**), NRG1 (**M**), PGR (**N**), RAC1 (**O**), RAC1B (**P**), SLUG (**Q**), SRC (**R**) and TGFα (**S**). Results expressed as % of control (set to 100%) are the mean (±SEM) of nine samples out three independent experiments (24 hours) and the mean of six samples out two independent experiments (48 and 72 hours). No significant differences were found compared to the MOCK control.

Appendix 8F: Additional education

During this Honours Programme research year the following courses were taken:

- **Introductory Statistics Course**
  Faculty of Veterinary Medicine, Utrecht University
  Course providers: Jan van den Broek en Hans Vernooij
  December 8th and 9th 2014
- **Writing a Scientific Paper**
  Institute of Veterinary Research (IVR), Faculty of Veterinary Medicine, Utrecht University
  Course provider: Annemarie van der Zeeuw
  6 Friday mornings, April-June 2015
  3 ECTS